IEEE Access
Multidisciplinary | Rapid Review | Open Access Journal

Received December 17, 2018, accepted January 1, 2019, date of publication February 4, 2019, date of current version September 13, 2019.

Digital Object Identifier 10.1109/ACCESS.2019.2897212

The Spatial Singularity Expansion Method for Electromagnetics

SAID MIKKI[1], ABDELELAH M. ALZAHED[2], AND YAHIA M. M. ANTAR[3], (Life Fellow, IEEE)

[1]Electrical and Computer Engineering and Computer Science Department, University of New Haven, West Haven, CT 06516, USA
[2]Electrical and Computer Engineering Department, Royal Military College of Canada, Kingston, ON K7K7B4, Canada
[3]Electrical and Computer Engineering Department, Royal Military College of Canada, Kingston, ON K7K7B4, Canada

Corresponding author: Said Mikki (said.m.mikki@gmail.com)

ABSTRACT We develop a general singularity expansion method (SEM) focused on the spatial structure of electromagnetic fields and currents. In contrast to the traditional temporal SEM, where complex analytical continuation is performed on the forward Green's function of free space, we propose applying the SEM to the reverse Green's function of the electromagnetic device, the recently introduced antenna current Green's function, leading to the discovery of new current and radiation modes. The new spatial SEM turns out to depend only on single-frequency field/current measurement besides completely avoiding the problem of separating early- and late-time responses that have been hindering the traditional approach. The theory is first developed at a very general level and then applied in detail to 1-D wire antennas. We manage to express the far field in terms of the spatial-SEM modes in a closed analytical form. The theory is confirmed by directly comparing with the full-wave method of moment solutions, and excellent agreement between theory and numerical analysis was obtained for generic wire array configurations. The resulting spatial-SEM is expected to stimulate researches into a new generation of frequency-domain RCS target identification technologies and electromagnetic sensing by developing special algorithms relying mainly on the spatial structure of the fields and currents fed by measurements at single frequency instead of the time-domain data usually required in traditional SEM.

INDEX TERMS Singularity expansion method (SEM), Green 's functions, numerical methods.

I. INTRODUCTION

Since its proposal many decades ago, the Singularity Expansion Method (SEM) [1]–[7], [10]–[12] has enjoyed a tremendous popularity in both computational and applied electromagnetics due to its very generic character and numerical robustness. For example, it was applied to target identification [5] and numerous other antennas and scattering scenarios (see the recent survey [7] for more references and discussion.) For antenna systems, SEM also found its way into non-radar applications like current distribution synthesis and the efficient computation of multi-layer Green's functions, e.g., see [15]–[18]. The method continues to be very popular in the field of RCS measurement and characterization and various improvements and modifications in the main algorithm have been gradually introduced by the research community [21]–[33]. We note that the SEM can be applied to both antenna and scattering problems as the list of papers quoted above may suggest. Since this is a general spectral approach to the analysis of electromagnetic signals, the specific manner in which the field or data, i.e., whether in antenna or scattering mode, does not matter much. That explains why SEM has been generally one of the post powerful analytical, computational, and synthesis methods in applied electromagnetics.

However, the existing SEM is essentially a *time*-domain approach, where a temporal signal, say the measured radar echo, is probed in order to determine its deeper spectral composition, namely the time signal's *poles* and their *residues*. Although some information about the spatial distribution of the current enters into the traditional SEM expression through the theory of characteristic modes, e.g., see [12], [16], the SEM still extracts and is based on what amounts to essentially *temporal* electromagnetic information as indicated by the fact that the classical SEM expansion (reviewed below) is based on the Laplace transform. However, there is

The associate editor coordinating the review of this manuscript and approving it for publication was Mehmet Alper Uslu.

a need to investigate the natural and obvious generalization of the SEM to embrace *spatial* electromagnetics as well. The reason is that electromagnetic fields are spacetime processes in which the spatial and temporal degrees of freedom are subtly interwoven into each other. While a purely temporal SEM is readily available (the traditional multi-decade long approach cited above), to our best knowledge an explicit and systematic purely spatial SEM has never been developed in the applied electromagnetic literature.

The authors believe that a construction of a spatial SEM formalism is desirable for both theoretical and applied reasons. From the purely theoretical point of view, the spatial SEM is the next natural step needed before moving to the fully-fledged spatio-temporal formulation of SEM in electromagnetics (not available yet), so building a specific formulation focusing mainly on the spatial degrees of freedom, i.e., what we refer to here as the spatial SEM (S-SEM), can be considered a highly motivated attempt for fundamental reasons. On the other hand, the vast majority of *applied* electromagnetic problems, e.g., radar detection, target identification, antennas, etc, appear to directly involve spatial information, like the scatterer's geometrical shape, the radiated field focus, beamwidth, angle of incidence, and so on. Therefore, having at hand a deeper understanding of how electromagnetics and geometry interact through a spectral analysis conducted in the spatio-frequency domain can provide a rich framework for new generations of applications and algorithms. In fact, it seems that the proposed S-SEM algorithm does provide such indication since the authors were able to use simplified version of it to devise new electromagnetic machine learning algorithms for several types of applications, e.g., see [44]–[46].

The present paper provides three new contributions to the topic. First, we supply, to our best knowledge, the first integrated and focused formulation of the spatial-SEM as such. Second, we present the first formulation of the relation between radiation fields and the spatial-SEM poles. Indeed, it turns out that the far field is analytically expressible in terms of a linear superposition of basic radiation functions, which we call here spatial-SEM *radiation modes*. We also show how to obtain special spatial-SEM *current modes*. The relation between these spatial-SEM field and current modes is captured by a functional form reminiscent of an angular sinc function centered at the spatial-SEM pole location, an observation that is currently being exploited by the authors to design machine learning algorithms for inverse modeling applications of the theory. Third, we provide extensive numerical validation of the method for various wire antenna structures, involving bent wires and array configurations, including comparison with MoM.

The present work is organized as follows. Because of the complexity of the background needed in order to properly understand the proposed spatial SEM and in order to make the work available to the largest number of readers, we provide in Sec. II a special review of the background needed in order to understand the need to transition from temporal to spatial type SEM. In particular, Sec. II-A first reviews the Green's function of electromagnetics that forms the convenient setting for a correct foundational treatment of the subject. In Sec. II-A.1, we outline the familiar forward Green's function in free space, followed in Sec. II-A.2 by the inverse Green's function (ACGF). Indeed, we show that it is the latter what provides the natural stage for exhibiting and developing the spatial version of the SEM algorithm. Next, in order to motivate the new S-SEM method, we first review its forerunner, the temporal SEM (T-SEM) in Sec. III, where the theoretical foundations of the SEM are briefly highlighted in order to prepare for the transition to the spatio-frequency domain. This transition is initiated in Sec. IV, where the key ideas of the S-SEM are introduced for the simple case of scalar radiation. The comparison with the temporal SEM is then made visible there. In the next step, we move from the fully generic algorithm to a very concrete implementation for an actual electromagnetic scenario, in this case wire antennas. This example is chosen for its simplicity in implementation and mathematical analysis. Generalization to non-wire scatterers will be taken up in future papers but does not introduce essential new ideas in terms of general formulation. A core dimension of the S-SEM method is then presented in Sec. VI, which introduces a novel connection between the S-SEM data and the far field, leading to the discovery of new set of far-field radiation modes. The radiation field will then be expressed analytically in terms of the S-SEM data, with implications for gains on both the numerical and physical aspects. The S-SEM method is then verified by conducting extensive analysis of various wire structures. Selected examples are presented in Sec. VII, involving straight wires (symmetric and asymmetric excitation), two- and three- element wire arrays. Comparison was made with commercial MoM. Finally, we end up with conclusions mentioning some potential applications of the S-SEM method.

II. MOTIVATIONS AND BACKGROUND

Since the singularity expansion method is closely related to the Green's functions of electromagnetic problems, we need to first provide a quick review of the various types of such quantities in order to prepare for the transition to spatial SEM and also to understand the latter's relation to the traditional temporal SEM. This is because, as will be explained shortly, SEM is fundamentally connected with the Green's functions of electromagnetics. However, while the traditional *temporal* SEM is linked to the *forward* Green's function, the *spatial* SEM turns out to be related to the *inverse* Green's functions (the ACGF). Both types will be briefly reviewed in the next few paragraphs before moving to their connection with the SEM.

A. REVIEW OF FORWARD AND INVERSE GREEN'S FUNCTIONS IN ELECTROMAGNETICS

1) FORWARD GREEN'S FUNCTIONS

Consider a radiating current $J(r, t)$ (on an antenna, scatterer, combination of both) with support region V_s and enclosing

surface $S := \partial V_s$. We are interested in the electromagnetic fields produced by this source. The radiated electric field can be expressed in terms of the source current in operator form as [49], [59]

$$E(r,t) = \mathcal{L}_{rad}\left\{J(r,t)\right\}, \tag{1}$$

where $\mathcal{L}_{rad}$ is the radiation operator of the problem. This operator is linear, and hence one would expect that a Green's function of this operator can be found such that

$$\bar{G}(r,t)\cdot a = \mathcal{L}_{rad}\left\{a\,\delta(r,r';t,t')\right\}, \tag{2}$$

where δ is Dirac delta function, in general a 4-dimensional version. Here, the generic vector a provides the direction of the source current, while $b = \bar{G}\cdot a$ gives information about how the *response* of the system (radiation field) is oriented in space. One can think of the quantity $\bar{G}$ as a direct juxtaposition of two vectors in the form $b\,a$, which is referred to as a *dyadic* quantity.[1] Consequently, the Green's functions of electromagnetics are always dyadic.

It is well known that a Green's function satisfying (2) can be used to compute the radiated field due to any source through an equation of the form [35], [62], [63]

$$\mathbf{E}(\mathbf{r},t) = \int_{\mathbb{R}}\int_{V_s} \bar{\mathbf{G}}\left(\mathbf{r},\mathbf{r}';t,t'\right)\cdot\mathbf{J}\left(\mathbf{r}',t'\right)d^3r'dt', \tag{3}$$

where the t'-integral is performed over the entire real line $\mathbb{R}$ but is effectively restricted by causality to a lower limit (see for example [35].) Equation (3) is the familiar "convolution-type" expression of the principle of superposition in radiation problems: the total radiated field at any point in space-time is given by the sum of contributions emanating from infinitesimal dipoles located at volume element d^3r' and radiating within the time interval dt', summed over the entire source region V_s and all relativistically allowed time instants. Furthermore, because of the spatio-temporal shift-invariance of free space as an electromagnetic medium, the radiation response is insensitive to origins of space and time coordinates. For that reason, (1) and (2) can be replaced by

$$\bar{G}(r,t)\cdot a = \mathcal{L}_{rad}\left\{a\,\delta(r-r';t-t')\right\}, \tag{4}$$

and

$$\mathbf{E}(\mathbf{r},t) = \int_{\mathbb{R}}\int_{V_s} \bar{\mathbf{G}}\left(\mathbf{r}-\mathbf{r}';t-t'\right)\cdot\mathbf{J}\left(\mathbf{r}',t'\right)d^3r'dt'. \tag{5}$$

In other words, the response depends only on the spatial and temporal intervals $r-r'$ and $t-t'$.

In the frequency domain, a time harmonic excitation $\exp(j\omega t)$ is imposed (but not explicitly written). The angular frequency ω corresponds to the Fourier transform performed with respect to the temporal variation of the fields and currents. In this case, relation (4) and (5) become

$$\bar{G}(r-r';\omega)\cdot a = \mathcal{L}\left\{a\,\delta(r-r';\omega)\right\}, \tag{6}$$

$$\mathbf{E}(\mathbf{r};\omega) = \int_{V_s} \bar{\mathbf{G}}\left(\mathbf{r}-\mathbf{r}';\omega\right)\cdot\mathbf{J}\left(\mathbf{r}';\omega\right)d^3r', \tag{7}$$

[1]For background in dyadic algebra and calculus, see [53].

where here the frequency-domain quantities are given by

$$\begin{aligned}
\mathbf{G}\left(\mathbf{r}-\mathbf{r}';\omega\right) &= \int_{\mathbb{R}} \mathbf{G}\left(\mathbf{r}-\mathbf{r}';\tau\right)e^{-j\omega\tau}d\tau,\\
\delta\left(\mathbf{r}-\mathbf{r}';\omega\right) &= \int_{\mathbb{R}} \delta\left(\mathbf{r}-\mathbf{r}';\tau\right)e^{-j\omega\tau}d\tau,\\
\mathbf{J}\left(\mathbf{r};\omega\right) &= \int_{\mathbb{R}} \mathbf{J}\left(\mathbf{r};\tau\right)e^{-j\omega\tau}d\tau,\\
\mathbf{E}\left(\mathbf{r};\omega\right) &= \int_{\mathbb{R}} \mathbf{E}\left(\mathbf{r};\tau\right)e^{-j\omega\tau}d\tau.
\end{aligned} \tag{8}$$

For simplicity, in this paper we focus on radiating objects composed of materials supporting only the Perfect Electric Conductor (PEC) boundary condition.[2] In that case, only the electric field is relevant. Moreover, the radiating volume V_s can be replaced by the surface S enclosing this volume, after which equation (7) can be re-expressed more compactly as a surface integral in the form [54], [55]

$$\mathbf{E}(\mathbf{r};\omega) = \int_S \bar{\mathbf{G}}\left(\mathbf{r}-\mathbf{r}';\omega\right)\cdot\mathbf{J}\left(\mathbf{r}';\omega\right)ds', \tag{9}$$

Note that equations like (9) involving only surface integrals can still be written for radiation problems using the surface equivalence theorem [57], [59], [61]. Consequently, without loss of generality, in this paper all current distributions $J(r)$ can be assumed to be *surface* current density measured by A/m.

It is possible to explicitly solve the operator equation (4). Indeed, the *free-space forward* Green's function turns out to be [35], [49], [54], [62], [63]

$$\bar{\mathbf{G}}\left(\mathbf{r},\mathbf{r}';\omega\right) = \left(\bar{\mathbf{I}} + \frac{1}{\omega^2}\nabla^2\right)g\left(\mathbf{r},\mathbf{r}';\omega\right), \tag{10}$$

where $g\left(\mathbf{r},\mathbf{r}';\omega\right)$ is the frequency-domain *scalar* Green's function

$$g\left(\mathbf{r},\mathbf{r}';\omega\right) := \frac{e^{ik|r-r'|}}{|r-r'|}, \tag{11}$$

with the free-space wavenumber

$$k = \omega/c, \tag{12}$$

where c is the speed of light. For brevity, we sometimes write $r := |r-r'|$.

2) INVERSE GREEN'S FUNCTIONS

The previous discussion belongs to the *forward* Green's function formulation of electromagnetic radiation problems. There is, however, an equally important *distinct* Green's function essential for *antenna* (and scattering) problems, and that involves how known or given excitation *externally applied electromagnetic fields* induce a *current distribution* on the

[2]It is possible to generalize the proposed ACGF-SEM method to deal with non-PEC boundary conditions. However, the mathematical details of such extension appears to be quite complex and tedious though without essentially altering the main ideas of the method itself as presented in this paper. The authors will take up this generalization elsewhere.

antenna (or scatterer), which in turn will radiate according to the forward Green's function as in (9) and (10). The Green's function prescribing the transition from *field* excitation to *current* is called the *inverse Green s function.* On the other hand, the traditional Green's function of radiation physics in classical electrodynamics connecting *current source* with *radiated fields* is named (as before) the *forward* Green's function. To our best knowledge, the first proposal to classify electromagnetic problems to forward and inverse problems as described above was given by Schelkunoff [50] and Schelkunoff and Friis [51] in writings dating back to late 1940s, early 1950s. However, he did not actually formulate the idea of an inverse Green's function. Instead, Schelkunoff introduced the concept of *transfer admittance*, an *ad hoc* circuit approximation of continuous antenna structure, which was latter taken up by Harrington [58] in his early work on the Method of Moment (MoM) in the 1960s. The transfer admittance concept, however, remains an essentially discrete approximation of what is basically a *continuous* antenna problem. As initially given, there is no clear guarantee that the ever shrinking circuit segments into which the total antenna surface has been divided will lead to convergent results. Moreover, there was no exact derivation of the transfer admittance concept based on continuous electromagnetic operator theory. Finally, Schelkunoff's work does not seem to have attracted attention in the ensuing decades, and only examples involving wire antennas seem to have been published.

Nevertheless, such slow progress of research on the inverse electromagnetic (antenna) Green's function is not surprising given that the rigorous mathematical tools needed to construct an inverse Green's function of this type became widely available only after Schwartz's s pioneering work on distribution theory published in the early 1950s. Moreover, because of the rise of full-wave numerical electromagnetic solvers (MoM, FDTD, FEM, et), the general attention has gradually shifted toward direct discretization methods of boundary-value problems, rather than indirect techniques such as the Green's function method.[3]

This open research problem, i.e., broadly speaking, constructing a general inverse Green's function formalism valid or generic radiating structures, was taken up recently in a series of papers and monographs [36]–[40], [42]–[43]. In particular, it was shown that a special tensor-like *distribution* (generalized function), *the antenna current Green's function*, hereafter will be denoted by $\bar{\mathbf{F}}\left(\mathbf{r},\mathbf{r}'\right)$, exists such that the surface current distribution generated on an antenna with arbitrary surface S in response to an equally arbitrary illumination field $\mathbf{E}$ can given by [38], [43]

$$\mathbf{J}\left(\mathbf{r};\omega\right)=\int_{S}\bar{\mathbf{F}}\left(\mathbf{r},\mathbf{r}';\omega\right)\cdot\mathbf{E}\left(\mathbf{r}'\right)ds', \tag{13}$$

[3]In theoretical physics, the situation is exactly the opposite. Since the 1950s, the Green's function method has become a very prominent solution technique in fields like quantum field theory, condensed-matter physics, and material science.

where the integration is now performed on a the entire general antenna surface S. The proof of (13) required a special treatment involving ideas borrowed from functional analysis, distribution theory, differential geometry, all applied to integro-differential operator formulation of radiation problems [43].

Formally, the ACGF $\bar{\mathbf{F}}\left(\mathbf{r},\mathbf{r}';\omega\right)$ is defined by the following operator equation

$$\bar{\mathbf{F}}\left(\mathbf{r},\mathbf{r}';\omega\right)\cdot a=\mathcal{L}^{-1}\left\{a\delta_{L}\left(\mathbf{r},\mathbf{r}'\right)\right\}, \tag{14}$$

where $\delta_L\left(\mathbf{r},\mathbf{r}'\right)$ is a special surface delta function tangential to the antenna surface L whose precise construction can be found in [43]. $\mathcal{L}$ is the electromagnetic operator of the antenna connecting the (tangential) radiated field E to the surface current J through the integro-differential operator equation

$$E=\mathcal{L}J. \tag{15}$$

Explicit formulas and derivations of (15) can be readily found in literature, e.g., see [49], [57]–[61], [70].

The operator inversion (14) leading to the ACGF was shown to be possible in general by actually constructing the ACGF through a sufficiently generic sequential distributional series [43]. It was also shown in [37], [39], and [43] that a generalized reciprocity theorem exists, which relates the ACGF of the Tx antenna to the ACGF of the Rx antenna. In other words, if the same antenna is used to receive and transmit signals, then its Tx mode ACGF can be used to predict the Rx signal using the relation

$$\mathbf{J}_{Rx}\left(\mathbf{r}_{Rx};\omega\right)=\int_{S}\bar{\mathbf{F}}_{Rx}\left(\mathbf{r}_{Rx},\mathbf{r}';\omega\right)\cdot\mathbf{E}\left(\mathbf{r}'\right)ds', \tag{16}$$

where

$$\bar{\mathbf{F}}_{Rx}\left(\mathbf{r}_{Rx},\mathbf{r}';\omega\right)=\bar{\mathbf{F}}_{Tx}^{T}\left(\mathbf{r}',\mathbf{r}_{Rx};\omega\right). \tag{17}$$

In other words, the only operation needed to obtain the Rx mode ACGF from the Tx ACGF is merely switching the source and observation position variables and applying a dyadic transpose operation. This leads to considerable simplification of electromagnetic analysis since now only one type of inverse Green's function needs to be computed, that corresponding to a test Tx mode analysis.

The ACGF method has been also generalized to arbitrary multiple-antenna systems and was shown to include all information needed to compute the Rx signal with mutual coupling effects taken into consideration [43]. In general, for N-port Rx antenna, a total of N ACGFs is required, where the nth ACGF must have the following general form for arbitrary 2-dimensional antenna structures

$$\bar{\mathbf{F}}_{n}\left(\mathbf{r}_{n},\mathbf{r}'\right)=\sum_{l_1=1}^{2}\sum_{l_2=1}^{2}\hat{\alpha}_{l_1}\left(\mathbf{r}_{n}\right)\hat{\alpha}_{l_2}\left(\mathbf{r}'\right)F_{n}^{l_1\ l_2}\left(\mathbf{r}_{n},\mathbf{r}'\right), \tag{18}$$

for $n=1,2,...,N$. Here, $\hat{\alpha}_{l_1}(r_1)$ and $\hat{\alpha}_{l_2}(r_2)$ are two orthonormal vectors tangential to the antenna surface at positions r_1 and r_2. Therefore, *the dyadic ACGF has a restricted 3-dimensional dyadic form since all dyadic combinations*

appearing in the 3×3 *matrix must come from the* 2×2 *dyadic form conforming to the expression* (18). This fundamental general fact about ACGF dyadic forms, which sets them in direct contrast to the traditional Green's functions of electromagnetics, has been discussed in more details in [43] together with implications for theory and computations.

In this paper, we focus for simplicity on 1-dimensional antennas to illustrate the proposed ACGF-SEM method. More specifically, the implementation and actual numerical examples illustrating the spatial SEM will involve thin-wire antenna types as will be shown in Sec. V-A. In that case, the full restricted 3-dimensional dyadic form of the ACGF will not be needed since the problem can be effectively reduced to a single dyadic component in the form $\hat{\alpha}\hat{\alpha}$ because the tangent to the wire is always directed along the wire itself and is the same at every point (we focus on linear 1-dimensional antennas and avoid curved wires for simplicity. However, the ACGF formalism can deal with any curved radiating surface or wire, see [43].)

B. SEM AND GREEN'S FUNCTIONS

The SEM is a general method in computational and fundamental electromagnetics concerned with the temporal representation of various electromagnetic and source quantities via expansions of the form

$$\sum_n \alpha_n e^{s_n t}, \tag{19}$$

where both α_n and s_n are complex, usually duped *residues* and *poles*, respectively, and collectively will be referred to in this paper as the *temporal SEM data.* These data, i.e., residues and poles of time-domain currents or radiated fields, can provide valuable information about the geometric and material structure of the objects supporting or producing them, and hence their extreme importance in applied electromagnetics [1]–[33].

Early in its history, it was shown that the fundamental resonances unearthed by the SEM originate from pole singularities in the complex plane representation of the Green's function[4] $g(r, r'; \omega)$ encountered when attempting to solve the wave equation

$$u_{tt} - \nabla^2 u = 0 \tag{20}$$

using integral equation methods [12]. There, the main idea is to perform an *analytic continuation* of the well-known forward Green's function $g(r, r'; \omega)$ in order to extend it into a meromorphic function defined over the entire complex ω-plane. The *finite* number of poles of this extended function (in the lower half of complex plane) were found to constitute the SEM poles, while their residues correspond to the SEM residues.

Such classical understanding of the temporal SEM, however, had resulted in forcefully entangling the entire temporal SEM with the *forward* Green's function of electromagnetics $\bar{\mathbf{G}}\left(\mathbf{r}, \mathbf{r}'; \omega\right)$. Indeed, the classical SEM approach deals with the *temporal frequency* ω-dependence of the forward Green's function (10). Traditionally, this SEM technique uncovers singularities (and their coefficients) emerging from the *temporal* representation of the field attained via an inverse Fourier transform operations applied to frequency-domain data like (10). Consequently, only *one*-dimensional functions, most commonly *time* signals, can be analyzed through the traditional, i.e., *temporal*, SEM.

Because this classical SEM has been historically developed with an eye on its applications to radar and inverse modeling in electromagnetics, a physical interpretation of the SEM poles and residues was readily developed to explain the significance of the method in terms of the target's geometric data, e.g., size, shape, orientation, and so on [8]. Most successfully, what made temporal SEM very intuitively appealing was the association of *natural frequencies* corresponding to the SEM poles with internal multiple resonances caused by infinite back-and-forth-type wave reflections between two or more geometric singularities (corners, sharp edges, holes, etc) in the physical target's body. In that case, the *temporal* characteristics of the return echo would then reveal precious information about the geometric structure of the target, which may then be exploited later in order to develop novel applications such as high-fidelity target identification technologies.

Based on this *indirect* connection between the time-domain electromagnetic structure and the geometric structure, the authors believe it is now timely to inquire whether a *direct* connection between electromagnetics and the target's geometry exists. The most obvious possible connection is to consider the common factor between the two: *the spatial degrees of freedom.* Indeed, both electromagnetic fields and geometry share in the spatial structure of the problem, and hence it is very likely that a new SEM, a *spatial*-SEM approach, could provide direct and more enlightening information about the target's geometric composition. As will be shown in this paper, such approach turns out to be indeed feasible, with the key enabling theoretical concept *the Antenna Current Green's Function* that was introduced recently [38]. Indeed, in light of the *reverse* fundamental Green's functions of the antenna operator itself, the antenna current Green's function (ACGF) $\bar{\mathbf{F}}\left(\mathbf{r}, \mathbf{r}'; \omega\right)$, it is very natural to inquire into whether the basic intuition behind the conventional SEM, i.e., that applied originally to the *forward* Green's function $g(r, r'; \omega)$, can now be extended to the *reverse* electromagnetic Green's function $\bar{\mathbf{F}}\left(\mathbf{r}, \mathbf{r}'; \omega\right)$. This idea was first proposed in tentative form in [36] but had to wait to [39] until the details of ACGF formalism itself were carefully worked out in [38].

Therefore, instead of studying the *temporal* spectral structure of the forward Green's function $\bar{\mathbf{G}}\left(\mathbf{r}, \mathbf{r}'; \omega\right)$, the idea is to focus on the *spatial* Green's function of the antenna $\bar{\mathbf{F}}\left(\mathbf{r}, \mathbf{r}'; \omega\right)$, where the latter links arbitrary (not necessarily plane wave) illumination field to the response current

[4]That is, the Green's function of the scalar Helmholtz equation $\nabla^2 u + \omega^2 u = 0$.

excited on the antenna. Next, instead of studying the temporal frequency structure of the function $\bar{\mathbf{F}}\left(\mathbf{r},\mathbf{r}';\omega\right)$, we propose focusing on the *spatial* spectral content of the ACGF $\bar{\mathbf{F}}\left(\mathbf{r},\mathbf{r}';\omega\right)$ with respect to its $\mathbf{r}$-dependence. That is, the resulting spatial-SEM can also be considered a "spatial ACGF". It can be shown that the spatial-SEM provides a natural complement to the conventional SEM in the *spatial* domain, rather than being exclusively devoted to the time domain. In other words, *the spatial-SEM can be viewed as a single-frequency analog of the traditional multi-frequency temporal SEM in which the spatial SEM manifests itself as inherently multi-dimensional (because it applies to three spatial dimensions, while conventional SEM is only one-dimensional)*. In the remaining parts of this paper, this research program will be developed in details, where we first give a generic outline of the method using a simplified scalar mode, then provide detailed implementation for 1-dimensional structures. However, we first provide in Sec. III a quick comparison between the two distinct formulations of SEM in terms of space and time.

III. TRANSIENT SEM VERSUS SPATIAL SEM: THE GENERAL OUTLOOK

Before moving to the technical details of how to construct the proposed spatial SEM (hereafter, S-SEM) method, we first provide a general review of the classical transient (temporal) SEM (hereafter, T-SEM) with focuses on how the concept of the new S-SEM approach has been motivated by considerations arising from the classical SEM approach itself.

A. THE ORIGINAL FOUNDATIONS OF THE TRANSIENT SEM

In order to understand the origin of the spatial-SEM, we first present a very condensed review of the foundations of the classical transient-SEM. As was already shown by Ramm [11], [12], the SEM arises from attempts to solve the radiation problem in the time domain. This boundary/initial value problem involves solving the 3-dimensional wave equation. For simplicity, we restrict our discussion in this section to the *scalar* problem since the essential ideas are the same as in the full vectorial case.

The boundary/initial value problem boils down to finding a spacetime field $\Phi(r,t)$ satisfying

$$\frac{\partial^2\Psi\left(\mathbf{r},t\right)}{\partial t^2}-\nabla^2\Psi\left(\mathbf{r},t\right)=0;\quad \mathbf{r}\in\partial V,$$
$$\Psi\left(\mathbf{r},t\right)|_{t=0}=0,\ \Psi\left(\mathbf{r},t\right)|_{\mathbf{r}\in\partial V}=E(r),\qquad(21)$$

where $V\subset\mathbb{R}^3$ is the solution region and ∂V is its boundary surface. In this scalar model, the function $E(r)$, $r\in\partial V$, plays the role of "input excitation," while the scalar field Ψ is the spacetime response in the entire 3-dimensional region V. This model covers both antennas and scatterers.

Moving to the frequency domain, one obtains the Helmholtz equation boundary-value problem

$$\left(-\nabla^2+\omega^2\right)G\left(\mathbf{r}-\mathbf{r}';-\omega^2\right)=\delta\left(\mathbf{r}-\mathbf{r}'\right),\quad \mathbf{r}\in V,\qquad(22)$$

where $G\left(\mathbf{r}-\mathbf{r}';-\omega^2\right)$ is the 3-dimensional Green's function in the frequency domain. By transforming the problem to the Laplace domain via $s=i\omega$, the solution to (21) may be given by [11]

$$\Psi\left(\mathbf{r},t\right)=\frac{1}{i2\pi}\int_{c-i\infty}^{c+i\infty}\Psi\left(\mathbf{r},s\right)e^{st}ds,\qquad(23)$$

where

$$\Psi\left(\mathbf{r},s\right):=\int_V G\left(\mathbf{r}-\mathbf{r}';-s^2\right)E\left(\mathbf{r}'\right)d^3r.\qquad(24)$$

Here, the relation (23) is the (temporal) inverse Laplace transform of the "frequency-domain response" $\Psi\left(\mathbf{r},s\right)$. Note that this latter response is itself expressed as a "convolution-type" (linear superposition) integral (24) through the fundamental property of the Green's function method. The real frequency ω was transformed into the imaginary variable $s=i\omega$ in order to facilitate the method deployed in [12] for the purpose of proving the SEM expansion in the time domain. Indeed, the inverse Laplace transformation (23) is now treated as a contour integration in the complex s-plane. Using analytic continuation and residue theorem, it turns out that the general solution of (21) can be expanded as

$$\Psi\left(\mathbf{r},t\right)=\sum_{n=1}^{N}c_n\left(\mathbf{r}\right)e^{p_nt}+e_N\left(\mathbf{r},t\right)\qquad(25)$$

in the time domain, and

$$\Psi(r;s)=\sum_{n=1}^{N}c_n(r)(s-s_n)^{-1}+e_N(r;s)\qquad(26)$$

in the frequency domain. Here, the complex numbers p_n, $n=1,2,..,N$, are the *poles* of $G\left(\mathbf{r}-\mathbf{r}';-s^2\right)$. The function $e_N\left(\mathbf{r},t\right)$ in (25) is an error function measuring the deviation of the sum over n from the true field Ψ. In the frequency domain, the quantity $e_N(r;s)$ is an entire function in the complex s-plane. Ramm [12] provided sufficient conditions ensuring that

$$\left\|e_N\left(\mathbf{r},t\right)\right\|\to 0\qquad(27)$$

for some proper function norm $||\cdot||$. In this case, the result (25) can be interpreted as the SEM expansion with p_n playing the role of poles and c_n their coefficients (residues.) The real challenge in theoretical SEM research is to show that the convergence (27) holds in general for sufficiently small SEM model order N and very generic antenna/scatterer geometry.

A major difficulty in applying the transient-SEM expansions (25) and (26) is the error function e_N, which cannot be equated to zero in general. It was shown early in the history of transient-SEM research that $e_N(r,t)$ can be interpreted as the "early time response" of the target, e.g., see [8]. Although that indeed does help in applying the T-SEM formula to practical settings, one *still* needs to distinguish and separate the early- and late-time responses in order to explicitly deploy the complex exponentials sum approximation of the basic

SEM (25). Lack of an adequate fundamental theoretical criterion through which such separation can be enacted *a priori* is one of the major difficulties in the traditional T-SEM formalism. As we will show shortly, *the proposed single-frequency (spatial) SEM does not suffer from this problem since its time-harmonic dependence* $\exp(i\omega t)$ *is factored out, motivated by the irrelevance of early and late time in steady state analysis in such single-frequency spatial (S-SEM) framework.* Indeed, *all known spatial-SEM expressions found by the authors so far involve only the complex exponentials sum series and no error function is needed.*

We may summarize the most important features of transient SEM (T-SEM) as follows:

1) The T-SEM involves Laplace transformation in the time domain. The inverse Laplace integral is then deformed into the complex plane by a process of analytic continuation.
2) The T-SEM is fundamentally based on the electromagnetic 3-dimensional Green's function of the scatterer/antenna problem.
3) The T-SEM uses analytic continuation and residue theorem to build the complex exponentials expansion of the field/current in the frequency domain. This is a theory of complex analysis in *one* complex variable.
4) T-SEM poles arise from the poles of the s-analytically continued complex Green's function $G\left(\mathbf{r}-\mathbf{r}';-s^2\right)$.
5) The T-SEM poles coefficients are the *residues* of this complex function (extended into the entire complex plane) associated with those poles.

Note that all these features remain essentially unchanged when we move from scalar to full-electromagnetic vectorial formulation of the T-SEM and therefore will be taken as our main comparison points in the motivation for constructing a spatial SEM approach.

B. FUNDAMENTAL MOTIVATION AND TRANSITION TO THE SPATIAL-SEM METHOD

From Sec. III-A, we can clearly see that the transient SEM is fundamentally a time-domain approach to electromagnetic signals. However, since the main goal is discovering useful correlations between the signal (field, current, charge) and the *geometrical* structure of the object supporting or producing these signals (antennas, scatterers), then it is very natural to explore the potential of constructing a purely *spatial* SEM formalism. The intention would be finding out how rich information buried in the spatial structure of electromagnetic signals like radiation fields or current distributions are connected to the spatio-geometric structure of the targets, devices, or antennas. In particular, we ask:

1) Fundamental Electromagnetic Theory: Can we expand the spatial field/current function into complex poles? If so, what physical significance and engineering potential do they possess?
2) Electromagnetic Machine Learning: Can substantial geometrical information about the antenna/scatterer structure be efficiently extracted from those spatial-SEM poles? Most importantly, Can geometrical information be found by processing measured electromagnetic data like near- or far- fields?

The answers to these two questions is both YES, as will be demonstrated throughout what follows. Note, however, that the proposed spatial-SEM diverges completely from the transient SEM in most of the main features listed at the end of Sec. III-A: *the spatial SEM turns out to be a very different SEM approach with its own method of derivation and physical interpretation of its results and expressions*. The precise manner in which this difference with the classical transient SEM is manifested will be emphasized below.

IV. SPATIAL SEM: THE KEY IDEAS

Before we investigate how a spatial SEM can be constructed, a good preliminary starting point can be retracing the original formulation presented in Sec. III-A to see if certain aspects of that now classical derivation can be salvaged in a purely spatial formulation. To do this, we need a *Green's function in the spatial domain* to replace the s-domain $G\left(\mathbf{r}-\mathbf{r}';-s^2\right)$ employed in deriving the T-SEM relation (26). A proper spatial Green's function structure was introduced only very recently and reviewed in Sec. II, where one may readily see that the situation in regard to the electromagnetic Green's functions in *space* is considerably more complex than the corresponding case in the time domain case. Indeed, as was discussed in Sec. II, there are two fundamentally distinct types of Green's function in applied electromagnetics, the forward and inverse functions discussed in Sec. II-A.1 and II-A.2, respectively. It will be shown that doing SEM in *time* requires working with the *forward* Green's function (free-space dyadic Green's function), while working with SEM in *space* is possible through the *inverse* Green's function (ACGF).

A. THE GENERIC APPROACH: A SIMPLIFIED SCALAR MODEL

In order to present a simplified introduction to the complex subject of how the spatial electromagnetic Green's functions interact with the spatial SEM, we develop in what follows a *scalar* (acoustic) electromagnetic model of the ACGF. Note that strictly speaking all electromagnetic radiation problems must involve a tensor-type or dyadic Green's functions. However, for the purpose of presenting the main ideas, the following scalar formulation is sufficient. A generalization to 3D tensors for one-dimensional antennas will be given in Sec. V, while the formulation for two-dimensional antennas will be tackled elsewhere.

First, we recall from Sec. II there exists two Green's, one function connecting input *field* excitation $E(r;\omega)$ with the radiation field $\Psi(r;\omega)$, i.e., via the ACGF. Let a "scalar ACGF" be denoted (for scalar problems) by $F(r,r')$. Strictly speaking, every component of the full dyadic ACGF form, namely once of the functions $F^{l_1 l_2}(r,r')$, can be referred to generically by this "scalar ACGF" $F(r,r')$. From now on and until the end of the present section, we implicit understand

by the scalar problem nothing other working with only *one* of the nine dyadic components of the full ACGF dyad 18. The electromagnetic problem will always by vectorial and hence the Green's function (and the spatial-SEM) will require a dyadic treatment. Therefore, the S-SEM expansion to be described below will have to be repeated for every independent dyadic component. Consequently, and in order to simplify the presentation, only a generic ''scalar ACGF'' case is presented in this section.

The next step is to replace the original ACGF main relation (13) by the following ''scalar ACGF'' formula

$$J(\mathbf{r};\omega) = \int_{\partial V} F\left(\mathbf{r},\mathbf{r}';\omega\right) E\left(\mathbf{r}';\omega\right) ds, \tag{28}$$

which connects the scalar excitation field $E(r;\omega)$ with the scalar source $J(r;\omega)$ induced on the antenna/scatterer. Here, the integration is 2-dimensional and is performed over ∂V, the antenna/scatterer's surface. The scalar quantity $J(r;\omega)$ is interpreted as a surface density source distribution.

For the purpose of introducing the generic S-SEM, we will use (28) in this section to explain the method. However, the reader should recall that (28) is *not* obtained from (13) as one component of the latter at a time. Indeed, the dyadic product in the integrated of (13) means that every individual component of the surface current J induced on the antenna by the excitation field E will involve a *linear superposition combination* of several scalar equations like (28). However, the key ideas to be introduced shortly will remain unaffected by that since each component of (13) can still be expanded using the S-SEM series of (28) given below.

For completeness, we also mention the second Green's function, i.e., the standard *forward radiation Green's function of free space*, here denoted by $G_{rad}(r,r')$, where we have

$$\Psi(\mathbf{r};\omega) = \int_{\partial V} G_{rad}\left(\mathbf{r},\mathbf{r}';\omega\right) J\left(\mathbf{r}';\omega\right) ds, \tag{29}$$

through which the final radiation field $\Psi(\mathbf{r}), r \in \mathbb{R}^3 - V$, is obtained from its source $J(\mathbf{r}), r \in \partial V$.[5] The relation (29) can be thought of as the scalar version of (9) in the same way in which (28) is the scalar version of (13).

Most importantly for the spatial-SEM proposed here, it turns out that there is *no* need to operate with the full spatial Green's function connecting the input field excitation $E(r,t)$ with the radiation field $\Psi(r,t)$. Indeed, the problem can be considerably simplified if the following two directives are adopted:

1) To build a spatial SEM, focus only on the spatial degrees of freedom. More specifically, we operate with time-harmonic fields and obtain single-frequency results where all spacetime sources and fields effectively reduce into 3-dimensional spatial functions.
2) We decompose the spatial Green's function (the electromagnetic response function) into two parts, the forward and inverse Green's functions (see Sec. II.) The basic spatial-SEM will be applied to the first component only, i.e., the device/object Green's function.

Directive (1) implies that the spatial SEM approach proposed here will lose *temporal* information. In spite of this, the advantages in our opinion are considerable since the structure of the method will acquire greater simplicity if we focus only on space, i.e., work with a space-frequency formulation of the electromagnetic problem. It is possible, though, to combine spatial and transient SEM in the future, leading to a kind of ''spacetime SEM,'' even though the connection between time and space here is still not well understood.

Directive (2) implies that the spatial-SEM's focus is on the spatial degrees of freedom of the *source*, i.e., the current producing radiated or scattered fields. The spatial-SEM poles and their coefficients to be introduced below will all characterize the spatial current produced on the object. Later in this paper (Sec. VI) we will show that a very direct relation between the fields and the current exist. In fact, we show that every spatial-SEM pole will excite a special far-field ''natural radiation mode'' with a closed form analytical formula connecting the radiation pattern with the spatial-SEM data.

B. DIRECT CONSTRUCTION OF THE SPATIAL SEM: AN INITIAL GENERIC APPROACH

Based on this general analysis, we expand the functional dependence of the ACGF $F(r,r;\omega)$ on r into a finite number of complex exponentials. To achieve this, we restrict the region over which the ACGF or the current is defined to a set of M *compact* nonoveralpping domains $U_m, m = 1,2,..,M$, hereafter duped *spatial-SEM patches*, covering the entire antenna's surface ∂V. These patches exhibit rough similarity to the coordinate patches deployed in the exact construction of the ACGF found in [43], which in turn was ultimately founded on the fact that ∂V is a 2-dimensional Euclidean manifold. However, the difference between the coordinate patches there and the SEM patches U_m introduced here – in addition to the fact that U_m are nonoveralpping while coordinate patches are – is that in U_m we explicitly take into account that the manifold ∂V has *boundary* (''edges'' or ''sharp sides.'') There are, however, more fundamental difference between the SEM parch division here proposed and others found in literature like MoM and the original ACGF method. Few of these issues will be discussed below but more details will be given elsewhere.

First we note that the current distribution normal to a physical edge is known to be zero [57] (we assume zero thickness layer and ignore effects like singular charge accumulation at nonsmooth corners and current flow over caps and round edges). Hence, we may assume that for the S-SEM consideration, a given current component under consideration decays to zero if part of the boundary of ∂V is included in U_m. (This fact will be crucial for ensuring that the spatial-SEM series, e.g., equation (35) below, will always converge with

[5] One can view the complete transfer function connecting the input excitation to the produced field as the *cascade* connection of two distinct, fully independent Green's function, one characterizing the device or the scattering object, i.e., the ACGF $F(r,r';\omega)$, while the other is the free-space radiation Green's function $G_{rad}(r,r';\omega)$, a universal property of the radiation medium shared by all devices or objects.

negligible error function.) However, we note that in contrast to MoM and ACGF, we need in general to use *different* mesh divisions for different current component.

To see this, consider a division of the antenna surface into a partition where every patch includes an edge. As a basic example, consider the rectangular patch of Fig. 1. Every surface current can be expanded locally into the sum of two linearly independent current components (usually orthonormal) [57]. Let us call these components the "vertical" and "horizantal" components, respectively. Moving to the ACGF, we can assume that every component of the ACGF dyadic $F^{l_1 l_2}(r, r')$ in (18) can be expanded over different mesh, depending on how the corresponding current components

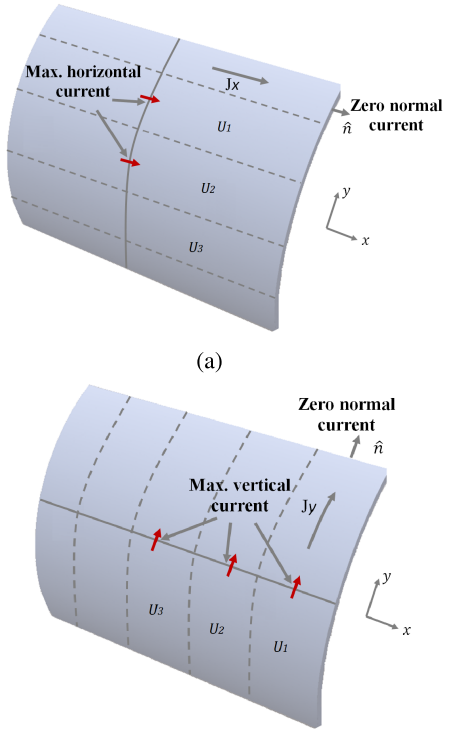

FIGURE 1. An example of a division of an arbitrary antenna surface into a collection of nonoverlapping patches, each including one physical edge (here, *physical edge* means either an edge segment on either the inner or our circumference.) The current component on each patch is zero in the direction to the patch's physical edge. In general, the total current distribution on the antenna will also include components parallel to the edge, and those can be non-vanishing. In that case, another set of patch divisions can be introduced such that those current components also decay to zero along perpendicular edges. The spatial SEM expansion will be comprised then of two sub-expansions, each corresponding to one current component. Since an arbitrary surface current on a 2-manifold can always be decomposed into two local linearly independent current components, this spatial SEM patch division scheme can always be implemented for arbitrary antennas. Here, we assume that the current can be expanded into two orthonormal components, referred to as "vertical" and "horizantal" components, with corresponding S-SEM mesh subdivisions given by (a) and (b), respectively. Note that the beginning or each patch cell U_m is chosen such that the current tend to be maximal at that internal edge (solid line). In this figure, curved patches will require curvilinear coordinates, so the x, y labels mentioned here should in general be understood as local coordinate systems. For the case of flat patches, local and global frames coincide.

are behaving with respect to the physical edge (i.e, whether we effectively have a "vertical" or "horizantal" current component.)

We may then expand every ACGF component on the SEM patch U_m (or also directly the scalar surface source J, see below) into a series of complex exponentials as follows

$$F_m\left(\mathbf{r}, \mathbf{r}'; \omega\right) = \sum_{n=1}^{N} \alpha_{nm}\left(\mathbf{r}'\right) e^{\mathbf{k}_{nm}(\mathbf{r}')\cdot\mathbf{r}} + e_{m,N}\left(\mathbf{r}'; \omega\right), \quad (30)$$

where $\mathbf{r} \in U_m$, $m = 1, 2, ..., M$ while k_{mn}, $n = 1, 2, .., N$ are tangential to U_m. For simplicity, we have dropped out explicit superscripts like l_1 and l_2 in (18) since for 2D problems we are interested in the main ideas mainly.

From the numerical viewpoint, the expansion (30) can be computed using Prony's method [67] or the matrix-pencil algorithm [68], [69]. Here, similar to T-SEM, N is the order of the S-SEM model. Again, e_N represents the "error" of this complex exponentials representation. The complex vectors $k_{mn}(r')$ and the complex numbers $\alpha_{mn}(r')$ are spatial-SEM poles and their coefficients, respectively, obtained when a delta source excitation is applied at the location $r = r'$ (because we are dealing with the current Green's function which requires this special excitation type, see Sec. II-A.2 and [43].)

We emphasize again that the expansion (30) can also be applied directly to the total *surface source distribution*, i.e., not only to the ACGF. The main *formal* difference between working with current or ACGF in the S-SEM is that in the former case neither k_{mn} nor α_{mn} will depend on r'. The disadvantage of working with currents instead of ACGF is that the spatial SEM based on the former becomes completely dependent on how the antenna or the target were originally excited. On the other hand, and as will become increasingly clearer below, by formulating the spatial SEM using the ACGF, the obtained SEM pole/coefficient data become truly general since they are independent of how the object under consideration was energized. Such generality and independence could lead to improved results in applications like radar target identification and inverse modeling since in various real-life scenarios it is not known what field excitation did interact with the object in the first place.

Now, by utilizing a proper mesh for each current/ACGF component as explained above and illustrated in Fig. 1, we may assume that both the current/ACGF decays to zero at the proper physical edge associated with U_m. Consequently, we can always find a direct numerical procedure to select k_{mn} and α_{mn} such that the error function $e_{m,N}$ gets as small as possible for sufficiently large N. For example, the popular matrix pencil method [68], [69], Prony's method [67], or even just brute-force optimization, can all be used to find a set of complex poles k_{mn} and coefficients α_{mn} ensuring that the error $e_{m,N}$ in (30) is small. Consequently, (30) will be rewritten as

$$F_m\left(\mathbf{r}, \mathbf{r}'; \omega\right) = \sum_{n=1}^{N} \alpha_{nm}\left(\mathbf{r}'\right) e^{\mathbf{k}_{nm}(\mathbf{r}')\cdot\mathbf{r}}, \ \mathbf{r} \in U_m, \quad (31)$$

at which the error function $e_{m,N}$ is explicitly dropped out. The relation (31) is our main generic spatial-SEM formula and should always be considered as an approximation of the otherwise *exact* ACGF. A relation similar to (31) can also be constructed for a generic current component.

For completeness, we give the total ACGF expansion on the entire antenna's surface as follows:

$$F^{l_1 l_2}\left(\mathbf{r}, \mathbf{r}'; \omega\right) = \sum_{m=1}^{M} \sum_{n=1}^{N} \alpha_{nm}^{l_1 l_2}\left(\mathbf{r}'\right) e^{\mathbf{k}_{nm}^{l_1 l_2}(\mathbf{r}')\cdot \mathbf{r}}. \tag{32}$$

That is, we here include the full component information (l_1, l_2) as described in (18) and also make the S-SEM data (α, k) explicitly dependent on those indices. Like (31), this expansion neglects the error functions in (30) but is moreover based on the fact that the SEM patches U_m are non-overlapping.[6]

If the current normal to the edge does not go to zero, e. g. because the edge is not well defined or not sharp enough, or because some special treatment of the transition between two sides on the same object is needed (e.g., the need for special "junction basis functions" as in FEM and MOM), it is still possible to apply the proposed spatial-SEM method but after some modification. Indeed, we first expand a generic current (or ACGF) component into a suitable set of basis functions as follows

$$f_m(r), \;\; r \in U_m, \; \forall m = 1, 2, ..., M, \tag{33}$$

where in each patch the basis function $f_m(r)$ goes to zero at its associated edge. In this case, there is no need for the spatial-SEM patches to actually contain the real physical edge of the structure, but each patch, including interior ones, possesses its own fictitious edges enclosing the basis function's own domain of definition. In such situation, we write the total current/ACGF component as

$$J\left(\mathbf{r}\right) = \sum_{m=1}^{N} a_m f_m\left(\mathbf{r}\right), \tag{34}$$

where we still assume that the basis functions' domains U_m are nonoveralpping. Afterwords, the mth basis function is expanded using the spatial-SEM expansion (31) in the following manner:

$$f_m\left(\mathbf{r}\right) = \sum_{n=1}^{N} \alpha_{nm}\left(\mathbf{r}'\right) e^{\mathbf{k}_{nm}(\mathbf{r}')\cdot \mathbf{r}}, \mathbf{r} \in U_m, \tag{35}$$

after which an equation similar to (31) can be written. In this paper, a basis-dependent formulation like (35) will not be necessary since we work mainly with 1-dimensional problems whose U_m are trivially the entire wire segment itself. Generalizations to 2-dimensional objects will be taken up somewhere else.

[6]Even, if there is an overlap, it is still possible to obtain a general expansion using partition of unity techniques borrowed from differential topology. For simplicity, we assume that such non-overlapping partition is always possible. For 1-dimensional problems, this is indeed the case, while for higher dimensions achieving this requires some additional work.

Finally, note that the SEM data $k_{mn}(r')$ and the complex numbers $\alpha_{mn}(r')$ in the generic spatial-SEM expansion (30) depend on the subdivision of the antenna surface into patches. This is not surprising since the pole $k_{mn}(r')$ measures the internal (spatial) resonances associated with the particular patch U_m. While the antenna's surface can be divided in infinite number of ways, it can be shown that *global* geometrical and topological information, like the shape, genus, and size of the antenna or target, can be recovered from measured electromagnetic data using special machine learning algorithm to be introduced by the authors elsewhere.

C. THE SPATIAL-SEM ALGORITHM

We provide a summary of the general spatial-SEM approach before moving into the more technically detailed part of our work. The generic S-SEM algorithm is shown in Algorithm 1. The 1-dimensional version of this algorithm will be developed in full in Sec. V-B.

Algorithm 1 The Generic S-SEM Algorithm for Antennas

1: Find the ACGF $F(r, r')$ of the antenna whose total surface is S. (This step is not effectively part of the S-SEM algorithm itself but is included here for convenience.)
2: Divide the entire antenna surface S into a set of nonoverlapping compact regions U_m, $m = 1, 2, ..., M$, such that each patch U_m contains a portion of the edges of S.
3: Assign to each patch U_m the current or ACGF component that vanishes normally at the antenna edge contained in U_m. (In other words, all current/ACGF patches have values of currents equal to zero at the edge, see Fig. 1.)
4: If needed, obtain another set of patch divisions U'_m for other current/ACGF components (since in general at most two linearly independent current components are needed to represent an arbitrary current distribution on a 2-dimensional surface.)
5: Expand the $\mathbf{r}$-function of the current (or the ACGF) into a series of finite complex exponentials using (31)

$$F_m\left(\mathbf{r}, \mathbf{r}'; \omega\right) = \sum_{n=1}^{N} \alpha_{nm}\left(\mathbf{r}'\right) e^{\mathbf{k}_{nm}(\mathbf{r}')\cdot \mathbf{r}}, \; \mathbf{r} \in U_m.$$

From this expansion collect the S-SEM data: the complex poles $k_{mn}(r')$ and the complex coefficients $\alpha_{mn}(r')$, for r' and all patches U_m, using a proper method, e.g., Prony's or matrix pencil methods.
6: Change r' and repeat the steps above to update the SEM data $k_{mn}(r')$ and $\alpha_{mn}(r')$.
7: Stop when the entire port region U_p (the region on S where the input antenna excitation field is applied) has been already scanned by $r' \in U_p$.

So far, the proposed spatial SEM has been intentionally generic and still not fully electromagnetic since all quantities dealt with so far are scalar, a choice deliberately made in order to ensure simplicity in presentation. Using the surface equivalence theorem, one can show that the ACGF and the

general spatial-SEM have dimensions at most equal to 2. Therefore, the full electromagnetic case will correspond to the 2-dimensional spatial-SEM, which is beyond the scope of the present paper but does not require any fundamentally new idea and will be reported elsewhere. Also, though the generalization to scattering is tedious, it is relatively transparent and will be treated in the future. In the remaining sections of this paper, we develop the spatial SEM algorithm in full details for the special case of 1-dimensional radiating antenna structures.

D. SUMMARY OF DIFFERENCES BETWEEN THE SPATIAL-SEM VERSUS THE TRANSIENT-SEM

Our main observations on how the spatial and transient SEMs differ are:

1) The T-SEM is fundamentally a time-domain approach, while the proposed S-SEM is a single-frequency method. This makes the later easier to apply to experimental scenarios since time-domain measurement methods are more expensive and difficult than their frequency-domain counterpart.
2) In contrast to the T-SEM, here no Laplace or spectral transformation is needed. The S-SEM is not based on performing inverse Fourier or Laplace transforms.
3) The S-SEM is fundamentally based on the Antenna Current Green's Function, which is defined only on the device or object's surface. In contrast, the T-SEM is based on the radiation 3-dimensional Green's function defined on the entire exterior region.
4) The S-SEM does not use complex analysis (analytical continuation and residue theorem) in order to derive the S-SEM singularities and their coefficients, while this is the case with T-SEM. This will equip the S-SEM with greater flexibility since now the physical interpretation of the S-SEM poles would not necessary be tied up with the concept of a pole of meromorphic function in the complex plane as is the case in T-SEM.
5) The S-SEM does not suffer from the problem of identifying the late time response essential in T-SEM. The error function (proportional to the early-time response in T-SEM) can be dropped out if the bases functions over the S-SEM patches are chosen carefully as per Sec. IV-B.
6) The classical T-SEM expansion requires combining a theory of *characteristic current modes* with a theory of poles/residues. To see this, note that in (25), the total spacetime dependence of the field/current is written as multiplication of $c_n(r)$ and $\exp(is_n t)$. Although the quantities $c_n(r)$ came into being as *residues* resulting from evaluating a contour integration in the complex plane, they also possess a *second* meaning – stressed here by being functions of r – whereby they play the role of *characteristic modes* of the radiating current [14]. On the other hand, *S-SEM, being a single-frequency approach, does not require any theory of characteristic modes*. In fact, as will be advocated later, the S-SEM terms $\exp(ik_m \cdot r)$ themselves can be interpreted as a new characteristic current mode on their own in independence from the conventional modes usually linked with SEM in the classical time-domain formulation.

V. FUNDAMENTAL FORMULATION OF THE SPATIAL-SEM METHOD FOR LINEAR WIRE STRUCTURES

A. THE 1-DIMENSIONAL ACGF FORMALISM

We consider a thin-wire antenna supporting a current $\mathbf{J}(\mathbf{r}, t)$ radiating in infinite and homogeneous free space medium with dielectric permitivity ε_0 and magnetic permeability μ_0. The antenna is oriented along the direction of the vector $\mathbf{L}$ where L is the total length. A time harmonic excitation $\exp(-i\omega t)$ is assumed but not explicitly written for simplicity. Based on the general dyadic form of the ACGF (18), the frequency-domain ACGF of this antenna can be immediately written in the form

$$\hat{L}\hat{L}\, F\left(\mathbf{r}, \mathbf{r}'; \omega\right), \tag{36}$$

where $\hat{L} := \mathbf{L}/L$ is a unit length vector in the direction of the antenna. In other words, the ACGF of a linear wire antenna/scatterer acquires a very simple form: The entire ACGF dyad can be factorized in the form ab, something that cannot be true in general. For that reason, it is enough for our purposes here to work with the *scalar* function $F\left(\mathbf{r}, \mathbf{r}'; \omega\right)$ in (36).

Using (13) it is possible to deduce that an arbitrary tangential field excitation

$$\mathbf{E}_{ex}\left(\mathbf{r}'\right) = \hat{L} E_{ex}\left(\mathbf{r}'\right), \tag{37}$$

interacting with the antenna $\mathbf{L}$ produces an excited current given by

$$\mathbf{J}(\mathbf{r}) = \hat{L} \int_L F\left(\mathbf{r}, \mathbf{r}'\right) E_{ex}\left(\mathbf{r}'\right) dl', \tag{38}$$

where l' serves here as a local length parametrization of $\mathbf{r}' = \mathbf{r}'\left(l'\right)$ along the wire $\mathbf{L}$. The expression (38) is valid for arbitrary tangential field excitation $E_{ex}\left(\mathbf{r}'\right)$.[7]

B. THE ACGF SINGULARITY EXPANSION METHOD (SPATIAL SEM)

a concrete example of SEM-type approximation of the ACGF is given as follows. For any linear-wire ACGF of the form

[7]There is a fundamental difference between using the indirect ACGF technique to compute the Rx current $\mathbf{J}(\mathbf{r})$ and other direct numerical methods, say the Method of Moment (MoM). Indeed, in the latter, one has to create a special mesh dependent on the (spectral) wavelength-structure of the excitation field. The ACGF formula (38), however, is valid for *arbitrary* input fields with any wavelength composition whatsoever as was shown both mathematically and numerically in [43]. It remains true, though, that obtaining such ACGF could be a challenging computational or lab process. To our knowledge, only MoM-approximations of the ACGF has been reported so far although there are ongoing efforts to develop alternative numerical methods [70]. For simplicity, we focus in this paper on ACGFs obtained using a delta-source excitation through an accurate higher-order MoM [34]. An improved numerical approximation of the ACGF via the MoM can be found by the way of a special sequential distributional technique developed in [43].

(36), one can seek an expansion

$$F\left(\mathbf{r},\mathbf{r}';\omega\right)=\sum_{n=1}^{N}\alpha_n\left(\omega\right)e^{s_n(\omega)l}+e_N, \tag{39}$$

where here α_n, s_n, $n=1,2,..,N$, stand for the SEM *poles coefficients* and *poles locations*, respectively. Equation (39) may now appear as a mere special case of the more general result (30) obtained above.

Because of the 1-dimensional nature of the ACGF of wire antennas, the expression (39) looks rather similar to the transient SEM formula. However, this similarity is superficial. Indeed, in the familiar temporal SEM [5], the quantities α_n are often denoted *residues*, reflecting their mathematical origin in complex integration theory [12]. We avoid doing so here because, in contrast to the temporal SEM, the quantities α_n defined by (39) can be generalized to 2-dimensional current distribution functions, leading to doubly-indexed coefficients α_{mn}, while the latter can *not* be traced back to the complex integration theory rooted in 1-dimensional functions (time signals.)

The quantity e_N appearing in (39) represents the spatial-SEM error resulting from truncating the series to only N terms. No exact analysis of the behavior of e_N is reported here. Instead, we use brute-force numerical algorithms to obtain the expansion (39) with the smallest possible number of singularities N.[8]

C. APPLICATIONS TO TX AND RX ANTENNA ANALYSIS

It should be mentioned that the SEM data in (39) are not only frequency functions, but also depend on the source field excitation's location r'. That is, one needs to write

$$\alpha_n=\alpha_n\left(\omega;\mathbf{r}'\right),\, s_n=s_n\left(\omega;\mathbf{r}'\right), \tag{40}$$

but for simplicity we drop out ω and r' whenever no confusion is expected. In order to put this observation into perspective, we develop the expressions of both Tx and Rx signal using the spatial-SEM formula (39) stated above for wire antennas. For the Tx antenna case, from (38), (39), and (40), we find

$$\mathbf{J}_{\mathrm{Tx}}\left(\mathbf{r}\right)=\hat{L}\sum_{n=1}^{N}\int_L\alpha_n\left(\omega;l'\right)E_{\mathrm{ex}}\left(l'\right)e^{s_n(\omega;l')l}dl', \tag{41}$$

where we truncated the SEM expansion (39) into N terms. Here, l' is the local *source excitation* position on the antenna, while l stands for the *induced current* position on the same antenna. As we can see from (41), the explicit dependence of the SEM data α_n and s_n on the source position r' or l' has to be taken into account in computing the total induced current.

Application of the spatial SEM to *receiving* antennas is a little different. In order to see the complete expression of a Rx signal at a port located at r_p (l_p in local coordinates), we use (39) in (38) and then apply the inverse reciprocity theorem (17) in order to deduce

$$\mathbf{J}_{\mathrm{Rx}}\left(\mathbf{r}_p\right)=\hat{L}\sum_{n=1}^{N}\alpha_n\left(\omega;l_p\right)\int_L E_{\mathrm{ex}}\left(l'\right)e^{s_n(\omega;l_p)l'}dl'. \tag{42}$$

Comparing (41) with (42), we immediately notice that *although* both are rooted in the same fundamental ACGF theorem (38) and the spatial-SEM (39), the respective manners in which the Tx and Rx currents are generated are different in the two fundamental operational modes. Indeed, in the Rx formula (42), one needs to compute the SEM data α_n and s_n only at position r_p, i.e., the port location. This is done by measuring the Tx mode current when a delta source is applied at r_p, followed by invoking the inverse reciprocity theorem in order to obtain the Rx ACGF from the just measured Tx ACGF. On the other hand, in computing the Tx current via (41), we notice that one must know the SEM data α_n and s_n *over the entire source excitation domain (the support of the field E_{ex}.)* That is, one needs the global spatial functions $\alpha_n(\omega;l')$ and $s_n(\omega;l')$, where l' ranges over the full spatial support of $E_{ex}(l')$, in order to compute the value of the induced current at one antenna location l.

D. THE SPATIAL-SEM CURRENT MODES

We provide here a new interpretation of the spatial SEM current. In contrast to the classical time-domain SEM solution, the spatial-SEM is a *single-frequency spatial* approach that expands the fundamental Green's function of the antenna, its ACGF, into fundamental *spatial* current modes $\alpha_n\exp\left(s_nl\right)$. Indeed, by substituting (39) into (38), we find

$$\mathbf{J}\left(l\right)=\sum_{n=1}^{N}\mathbf{J}_n\left(l\right), \tag{43}$$

where

$$\mathbf{J}_n\left(l\right):=\hat{L}\int_L\alpha_n\left(l'\right)E_{\mathrm{ex}}\left(l'\right)e^{s_n(l')l}dl' \tag{44}$$

are the spatial-SEM *current modes*. Therefore, under any excitation field E_{ex}, the current induced on the wire can always be written as a superposition of fundamental current modes $J_n(l)$ given by (44). The same expression (44) also suggests that only knowledge of the SEM data (40) is needed in order to evaluate those currents for a given excitation field E_{ex}. In other words, the spatial-SEM holds a considerable advantage over the temporal SEM in being not tied up with a fixed type of excitation field like, for instance, plane waves or specific port wave. *Regardless to the details of how the antenna is excited, i.e., for any functional form $E_{ex}(l')$ whatsoever, the induced current can be written in terms of modes $J_n(l)$ that themselves are computable by (44) via only one set of measured SEM data, the functions $\alpha_n(l')$ and $s_n(l')$.*

On another hand, the now popular "theory of characteristic modes," [48] which – as mentioned above – is already closely connected with the classical (transient) SEM, is strongly sensitive to the antenna excitation method. This is because

[8] Rigorous analysis of the intrinsic 1-dimensional (i.e., temporal) SEM can be found in [12]. To our best knowledge, since its recent proposal in [39], the alternative spatial SEM has not received a rigorous error analysis in the mathematical literature.

it applies to the current, not the ACGF of the antenna. The spatial-SEM modes $\alpha_n \exp(s_n l)$, however, are not eigenfunctions of the exact antenna impedance operator as is the case with classical characteristic modes [47]. Instead, the modes $\alpha_n \exp(s_n l)$ are Laplace modes of the ACGF. The ACGF itself is the Green's function of the *inverse of the antenna's impedance operator. Being a Green's function, the input excitation is completely decoupled from the induced current, and hence modes like* $\alpha_n \exp(s_n l)$ *become free of the local details of how the antenna was energized, resulting in stronger connection between the global geometrical details of the antenna with the SEM data.*[9]

VI. THE SPATIAL-SEM RADIATION MODES

The next major step in the spatial SEM is to show how the SEM data buried in the radiator's current distribution are connected with its corresponding radiation field. It will be shown here that the far field can be expressed analytically in terms of the SEM data (40). Moreover, it turns out that the spatial-SEM leads naturally to the discovery of a new set of far-field basis functions, what we call here the spatial SEM *radiation modes*. Explicit expressions for these modes will be derived below for the case of linear wire antennas with arbitrary length and orientation. The machine learning approach to target identification and inverse modeling based on the spatial SEM depends crucially on the organic connection between the field and the current since we can easily measure the field or RCS. The training data set for the ML algorithm will then be based on the far field, while the analytical relation between this field and the SEM data to be given below will form the basis of the construction of the algorithm predicting the geometry of the target from measured field data.

A. DERIVATION OF THE RADIATION MODES: SINGLE ANTENNA CASE

For simplicity, we develop the SEM radiation field theory in terms of the current distribution instead of the ACGF. However, in order to establish a connection with the previous formulation in terms of the ACGF, we consider here only currents excited by the delta-gap source excitation

$$\mathbf{E}_{ex}(l) = \hat{L}\delta\left(l - l_p\right), \tag{45}$$

where $r_p = \hat{L} l_p$ is the port location. Those are very close to the exact ACGF of wire antennas. Expression (43) can then be reduced to

$$\mathbf{J}(l) = \hat{L}\sum_{n=1}^{N} \alpha_n\left(l_p\right) e^{s_n(l_p)l}. \tag{46}$$

[9]Nevertheless, one may still expect some connection between the two types of modes though this is no direct or immediate relationship. In fact, classical characteristic modes are closer to the current functions $J_n(l)$ than $\alpha_n \exp(s_n l)$, the reason being that the former already contain the method of the antenna excitation within it as exemplified by E_{ex} in (44).

We next deploy the (scaled) far-field radiation formula [35], [43]

$$\mathbf{E}_{rad}\left(\hat{r}\right) = \int_L \mathbf{J}\left(\mathbf{r}'\right)\cdot\left[\bar{\mathbf{I}} - \hat{r}\hat{r}\right] e^{ik\hat{r}\cdot\mathbf{r}'} dr, \tag{47}$$

where

$$\hat{r}(\theta,\varphi) := \hat{x}\cos\varphi\sin\theta + \hat{y}\sin\varphi\sin\theta + \hat{z}\cos\theta \tag{48}$$

is the radial unit vector $\mathbf{r}/\|\mathbf{r}\|$, $\bar{\mathbf{I}}$ is the unit dyad, and $k = \omega/c$, where c is the speed of light.

The goal now is to establish a deeper insight into the nature of the radiation field by adopting the viewpoint of the spatial-SEM current. Use of the current (46) in (47) leads to

$$\mathbf{E}_{rad}\left(\hat{r}\right) = \hat{L}\cdot\left[\bar{\mathbf{I}} - \hat{r}\hat{r}\right]\sum_{n=1}^{N}\int_L \alpha_n e^{ik\hat{r}\cdot\mathbf{r}'} e^{s_n l'} dl', \tag{49}$$

which after inserting $\mathbf{r}' = \hat{L} l'$ reduces to

$$\mathbf{E}_{\text{rad}}\left(\hat{r}\right) = \hat{L}\cdot\left[\bar{\mathbf{I}} - \hat{r}\hat{r}\right]\sum_{n=1}^{N}\alpha_n f_n(\theta,\phi;\mathbf{L},s_n), \tag{50}$$

where

$$f_n(\theta,\phi;\mathbf{L};s_n) := \frac{e^{\left(ik\hat{r}\cdot\hat{L}+s_n\right)L/2} - e^{\left(-ik\hat{r}\cdot\hat{L}-s_n\right)L/2}}{\left(ik\hat{r}\cdot\hat{L}+s_n\right)}. \tag{51}$$

In writing (51), we assume that the entire range of l in the local parametrization of the antenna vector $\mathbf{L}$ is the interval $-L/2 < l < L/2$. Note also that the SEM poles locations s_n and their coefficients α_n are both functions of r_p, which explains the explicit mention of r_p in the LHS of (51). Such dependence in the RHS was dropped for simplicity but it must always be recalled: the SEM data and the far-field SEM radiation modes are all strongly dependent on the location at which the antenna delta-source field excitation is applied. Later numerical results will confirm this prediction.

B. DERIVATION OF THE RADIATION MODES: MULTIPLE ANTENNA CASE

Finally, we need to generalize the results (50) and (51) to handle the general scenario when multiple wire elements are present. This is essential for the transition to the machine learning approach based on the spatial SEM formalism since the geometrical information of the target will be captured by finding the best wire grid that fits the geometrical form of the target based on field training data.

Fig. 2 shows the basic model we use. An arbitrary distribution of M thin wires is assumed, where for the mth wire the end position is given by r_m^0, while the orientation is along the unit vector $\hat{L}_m$. On each wire, a local position vector is given by

$$l_m := \hat{L}_m l, \tag{52}$$

where again l plays the role of a local length parameter on the wire. An arbitrary position on the mth wire can then be give

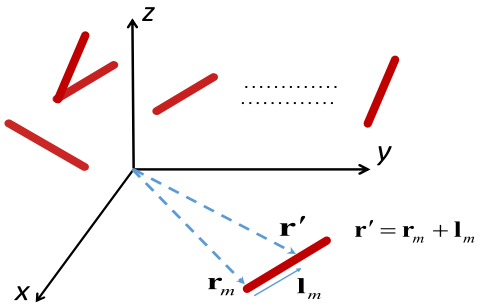

FIGURE 2. The geometrical model of an array of wires each locally traced by a position vector l_m.

by an expression of the form

$$\mathbf{r}' = \mathbf{r}_m^0 + \mathbf{l}_m = \mathbf{r}_m^0 + \hat{L}_m l. \tag{53}$$

Based on this geometrical model, the total current on the wire grid can be expanded as

$$\mathbf{J}\left(\mathbf{r}'\right) = \sum_{m=1}^{M} \hat{L}_m \sum_{n=1}^{N} \alpha_{mn}\left(r_{p,m}\right) e^{s_{mn}(l_{p,m})l}, \tag{54}$$

where the spatial SEM data s_{mn} and α_{mn} belong to the nth SEM pole of the current on the mth wire, while $r_{p,m}$ is the position where the delta source excitation is applied on the mth antenna.

The current (54) is now inserted into the radiation field formula (47), resulting in

$$\mathbf{E}_{\text{rad}}\left(\hat{r}\right) = \sum_{m=1}^{M} \hat{L}_m \cdot \left[\bar{\mathbf{I}} - \hat{r}\hat{r}\right] \sum_{n=1}^{N} \int_{L_m} \alpha_{mn} e^{ik\hat{r}\cdot\mathbf{r}'} e^{s_{mn}l'} dr'. \tag{55}$$

By performing a change of variables using (53), the integrals in (55) can be transformed into

$$\mathbf{E}_{\text{rad}}\left(\hat{r}\right) = \sum_{m=1}^{M} \hat{L}_m \cdot \left[\bar{\mathbf{I}} - \hat{r}\hat{r}\right] e^{ik\hat{r}\cdot\mathbf{r}_m^0} \times \sum_{n=1}^{N} \int_{L_m} \alpha_{mn} e^{ik\hat{r}\cdot\mathbf{l}'} e^{s_{mn}l'} dl'. \tag{56}$$

We now note that the integrals in (56) possess the same structure as (49), i.e., an integration performed locally on each wire. Therefore, we can immediately use the evaluations (50) and (51) to compute (56) as

$$\mathbf{E}_{\text{rad}}\left(\hat{r}\right) = \sum_{m=1}^{M} \hat{L}_m \cdot \left[\bar{\mathbf{I}} - \hat{r}\hat{r}\right] e^{ik\hat{r}\cdot\mathbf{r}_m} \times \sum_{n=1}^{N} \alpha_{mn} f_{mn}\left(\theta, \varphi; \mathbf{L}_m; s_{mn}\right), \tag{57}$$

where

$$f_{mn}\left(\theta, \varphi; \mathbf{L}_m; s_{mn}\right) := \frac{e^{\left(ik\hat{r}\cdot\hat{L}_m + s_{mn}\right)L_m/2} - e^{-\left(ik\hat{r}\cdot\hat{L}_m + s_{mn}\right)L_m/2}}{\left(ik\hat{r}\cdot\hat{L}_m + s_{mn}\right)} \tag{58}$$

The expressions (57) and (51) provide the most general form of the radiation field induced by a grid or array of radiating wires.

C. REMARKS ON THE RESULTS

The expansion (50) shows that the radiation field of a wire antenna can be always approximated by a superposition of basic radiation modes f_n where the expansion coefficients are precisely the spatial-SEM pole coefficients α_n. Each radiation mode $f_n\left(\theta, \phi; \mathbf{L}\right)$ depends on the excitation port location l_p, although we omitted this explicit dependence here for simplicity.

More remarkable is the manner in which each radiation mode shape is controlled by the pole's location s_n. Indeed, the radiation mode is a kind of "two-dimensional sinc" filter centered at the Re $\{s_n\}$ and Im $\{s_n\}$. (This can be readily seen if we plot $|f_n(\theta, \phi)|$.)

The spatial-SEM radiation modes (51) are not always orthogonal. By defining the intermodal correlation coefficient b_{nm} as

$$b_{nm}\left(\mathbf{r}_p, \mathbf{L}\right) := \int_{4\pi} f_n\left(\theta, \phi; \mathbf{L}\right) f_m\left(\theta, \phi; \mathbf{L}\right) d\Omega, \tag{59}$$

In general, it turns out that $b_{nm} \neq 0$, although the modes tend to become orthogonal when $|s_n - s_m|$ is large enough. This is an important distinction between the spatial-SEM modes introduced in this paper and the familiar eigenmode expansion method discussed in [12].

VII. VALIDATION OF THE DIRECT SPATIAL SEM ALGORITHM

In this section, we work toward providing a direct validation of the basic spatial SEM algorithm introduced above for 1-dimensional radiating structures. For simplicity, we work with the current distribution induced on thin wires by a delta-gap source. For our present purposes, this current is a good approximation of the wire's ACGF. Fig. 3 provides a simple schematic representation of a typical thin-wire model in electromagnetics. The wire antenna is modeled as a cylinder but

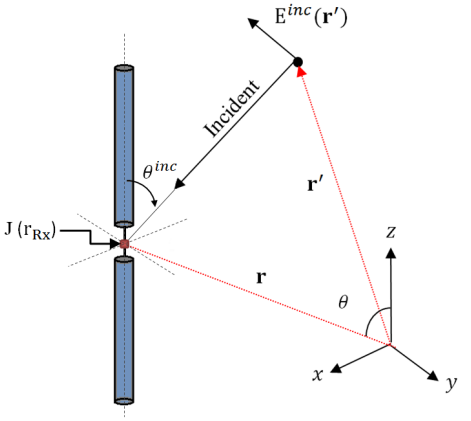

FIGURE 3. A schematic representation of thin-wire model of antennas in the Tx and Rx modes.

azimuthal variations in the current are ignored since these are essentially weak with the ratio of the wire length to radius is very large.

For the sake of establishing an independent reference to compare our results with, the spatial-SEM analytical expressions derived above were verified by direct comparison with full-wave simulation through the commercially-available Method of Moment (MOM) code WIPL-D [34]. Note that since commercial EM solvers don't usually offer non-standard excitation, the ACGF of the wire (if available) provides a more general approach to computing antenna characteristics going beyond existing commercial codes. Such non-standard methods of exciting antennas, however, will not be examined in what follows since here we are more interested in proof of concept of the basic spatial SEM approach.

As a first example, direct verification of the S-SEM algorithm will be given for two types of wire antennas, one excited with a delta-source gap applied at the middle of the thin-wire antenna system, while the second is energized by a source located off the midpoint. Both antennas are shown in Fig. 4. Each thin-wire antenna system has a total length of 0.5λ, where in the symmetric case (on the left) the two 0.25λ-half-wires can be connected with a load or voltage source, while the asymmetric case (on the right) involves a 0.45λ-wire connected to another 0.05λ-wire, also through a load or voltage source. The operating frequency of the designated systems is 1 GHz, which lies within a typical wireless antenna, radar or sensor frequency range. In conformity with the thin-wire approximation, the radius of the wire is very small compared with length, which allows us to ignore the circumferential component of the current distribution.

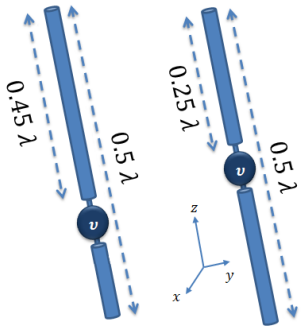

FIGURE 4. A schematic plot of two thin-wire antennas; it shows symmetric and asymmetric excitation of the wire.

Each single antenna is defined as two wires connected through a load or source. In other words, the spatial SEM expansion will be developed for each wire individually. The SEM surface partition U_m in our case consists then of two patches only for each antenna: one for wire#1 and another for wire#2. The current distribution will consequently always approach zero as we go toward the free end of the wire. In case multiple wires are used to build a more complex wire antenna structure, then there will be as many SEM patches U_m as there are wires. Each wire/patch will be joined to another through a junction consisting of either a source or load (we consider point junctions a special type of load.)

The MoM estimation of the antenna's current distribution induced by a delta source applied on the two antennas in Fig. 4 was analyzed using Prony's method in order to obtain S-SEM poles locations and coefficients. The S-SEM data obtained in this case are shown in Table 1 for the the symmetrically-excited antenna. As expected, only two complex conjugate pole pairs are needed to capture the current on the entire wire because it is known that resonant wires have current distributions that can be approximated by sinusoidal forms. In other words, the half-wavelength dipole represents a trivial example from the S-SEM viewpoint. In order to consider a more challenging example, the asymmetric wire in Fig. 4 is analyzed into its S-SEM data, shown in Table 2.

TABLE 1. Direct modeling S-SEM data for symmetric wire.

Wire	Poles	Residues
1	-4.384 + 15.3267i -6.4365 - 15.0244i	0.8338 - 8.0136i 6.416+ 3.7994i
2	6.4365 + 15.0244i 4.384 - 15.32671i	6.4161 + 3.7994i 0.8338 - 8.0136i
MSE	2.897×10^{-09}	

TABLE 2. Direct modeling S-SEM data for asymmetric wire.

Wire	Poles	Residues
1	0.3181-2.8225i -2.6681+1.2487i 2.3259+1.6317i	189.61-196.12i -228.38-79.434i 53.06+267.95i
2	0.0037-0.0053i -0.0037+0.0053i	20323+13472i -20323-13472i
MSE	2.736×10^{-09}	

The mean-square error (MSE) between the SEM current and the actual (MoM) currents is denoted by e_J and is also included in our analysis. The definition of e_J is

$$e_J := \frac{1}{L}\int_L |J_{\text{MoM}}(l) - J_{\text{S-SEM}}(l)|^2 dl, \tag{60}$$

where integration is performed over the entire antenna (multiple wires.) Both current components J_{MoM} and $J_{\text{S-SEM}}$ in (60) are tangential to their support wire. The two current distributions themselves are shown in Fig. 5, where excellent agreement can be observed.

It is worth stressing again that this entire analysis makes no use whatsoever of the distinction between late- and early-time response familiar in conventional, i.e., temporal, SEM. Indeed, all currents and fields oscillate harmonically in time with the same frequency. The spatial SEM method applies directly to the *entire* current distribution belonging to every patch, including an edge at which the normal component of the current vanishes. The key reason behind the lack of problems similar to early/late time response in S-SEM is that, contrary to the case of $t \to \infty$, we know all currents must become zero when their spatial arguments l goes to infinity. This can always be the case if the Algorithm 1 recipe

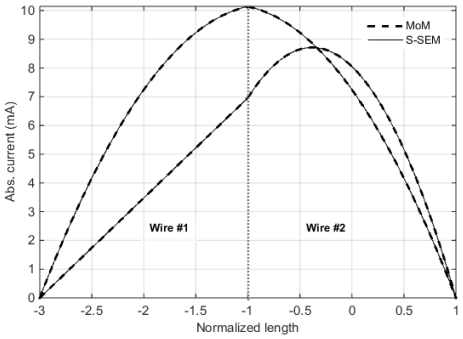

FIGURE 5. The plot shows a comparison between the EM solver, WIPL-D [34], currents and spatial-SEM currents given in [46]. The comparison is made for the symmetric and the asymmetric wire, where each element is assumed to be *two-wires* linked through the excitation source.

was followed by which the antenna's subdivision into non-overlapping regions U_m is enacted to ensure all tangential currents at the patches' edges are treated properly.

Note that the SEM data strongly depend on the location of the delta-source excitation, i.e., the position r' in the expressions (40) exactly as predicted by theory. This is why an asymmetrically-excited case was included here. In general, with nonsymmetric currents, the number of SEM poles needed to capture its *spatial* distribution increases compared with the symmetric case. For straight thin-wires, this is expected since the symmetric current is known to be close to a (spatial) sinusoid, which means that its SEM poles are trivial. This, however, is only a highly special case. In general, the spatial resonance structure of the current captured by its SEM data is highly complex and may require a large number of SEM poles to accurately capture subtle spatial current variations. Complicated geometrical shapes approximated by a large number of joined wires belong to cases of this type.

To now validate the spatial SEM field theory, the SEM data just obtained were inserted into the formula (50) in order to compute the far field without recourse to the radiation formula of classical antenna theory. The MoM code, on the other hand, uses precisely this classical radiation law in order to compute the field using the current distribution and the free space dyadic function [34]. A comparison between the far fields obtained using these two different methods are shown in Figs. 9(a),(b) for both the symmetric and asymmetric excitation. The very good agreement between the two confirms that the SEM radiation modes given in (51) does indeed capture the far field of an arbitrarily-excited straight wire antenna systems.

We next consider more complex antenna shapes. Fig. 6 shows an L-shaped antenna example designed in order to test whether the S-SEM current and fields can model changes in the direction of the current distribution described by the geometric length vector L. The L-shaped antenna is modeled by two equal-length arms joined at right angle. The system is excited by a delta-source concentrated at the corner of the antenna. The S-SEM model chosen here assigns different poles and coefficients to each wire in order to capture possible variations in the current at different parts of the

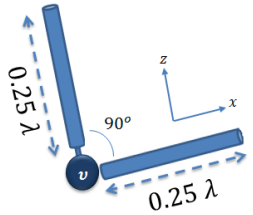

FIGURE 6. A schematic plot of an L-shape antenna.

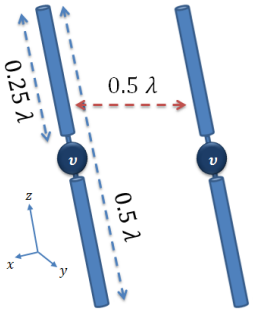

FIGURE 7. A schematic plot of a two-element antenna array with inter-element spacing of 0.5λ.

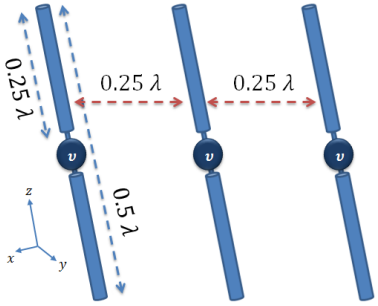

FIGURE 8. A schematic plot of a three-element antenna array with inter-element spacing of 0.25λ to act as a Yagi-Uda antenna.

TABLE 3. Direct modeling S-SEM data for L-shape wire.

Wire	Poles	Residues
1	-4.6262+15.1132i	5.9893 - 15.377i
	-6.1254-14.8853i	10.6519 + 11.635i
2	6.1254+14.8853i	10.6519 + 11.635i
	4.6262-15.1132i	5.9893 - 15.377i
MSE	7.214×10^{-09}	

system undergoing varying relative inclinations with respect to each other. As expected because of the symmetry of this special case, the currents are identical, but in general, more complex current distributions could be observed in more generic configurations. Table 3 shows the S-SEM data needed to represent the current in this case. Very good accuracy is observed.

To verify the S-SEM far-field theory, we use the formula (57), where the L-shaped is treated as an array of two elements coupled to each other at the corner. The previously

TABLE 4. Direct modeling S-SEM data for two-element array.

Wire	Poles	Residues
1	-4.4878+14.8977i -6.1912-14.6286i	4.4111 - 10.2636i 6.7716 + 7.994i
2	6.1912+14.6286i 4.4878-14.8977i	6.7716 + 7.994i 4.4111 - 10.2636i
3	-4.4878+14.8977i -6.1912-14.6286i	4.4111 - 10.2636i 6.7716 + 7.994i
4	6.1912+14.6286i 4.4878-14.8977i	6.7716 + 7.994i 4.4111 - 10.2636i
MSE	8.257×10^{-07}	

TABLE 5. Direct modeling S-SEM data for three-element array.

Wire	Poles	Residues
1	-3.8989+15.097i -6.8535-14.6382i	2.9407-5.7930i 3.5025+4.6380i
2	6.8579+14.6474i 3.8978-15.1065i	3.5027+4.6349i 2.9421-5.7908i
3	-3.7388+14.0213i -6.6165-13.4926i	5.8736-2.5082i -0.7675+5.6792i
4	6.6234+13.4947i 3.7336-14.0255i	-0.7677+5.6768i 5.8747-2.5065i
5	-3.8989+15.0971i -6.8535-14.6382i	2.9407-5.7930i 3.5025+4.6380i
6	6.8579+14.6474i 3.8978-15.1065i	3.5027+4.6349i 2.9421-5.7908i
MSE	2.356×10^{-08}	

TABLE 6. Inclination angle variation for L-shape wire.

Angle (degree)	MSE (Direct)	MSE (Reconstructed)
30	4.8348×-06	5.1984×-05
60	7.3487×-07	3.465×-06
90	7.214×10^{-09}	6.0427×-09
120	2.1772×-07	1.9814×-06

obtained S-SEM data in Table 3 are then used to compute the far field and the results compared with MoM. Fig. 9(c) shows excellent agreement between theory and MoM, indicating the ability of the S-SEM method to handle bent and complex wire antenna systems.

In order to investigate how the method works with separate elements, a simple two-element wire array is considered next. Fig. 7 illustrates the geometry of this case, where two symmetrically-excited half-wavelength dipoles are placed at distance 0.5λ of each other. The array is excited by two independent delta-gap voltage sources at the middle of each wire. Again, each antenna is treated as two separate wires, giving a total of four independent wires to represent the array system. The S-SEM data of this example are given in Table 4. Only two poles on each wire were needed. For asymmetrically-excited dipoles or more complex geometries, the number of poles in general increases and the S-SEM data become different on each wire. The far-field formula (57) is used to predict the far field analytically based on the data in Table 4. The comparison with MoM is given in Fig. 9(d) and again excellent agreement is observed.

Finally, we consider a three-element Yagi-Uda antenna system as shown in Fig. 8, with 0.25λ inter-element separation. For simplicity, the three element have equal length

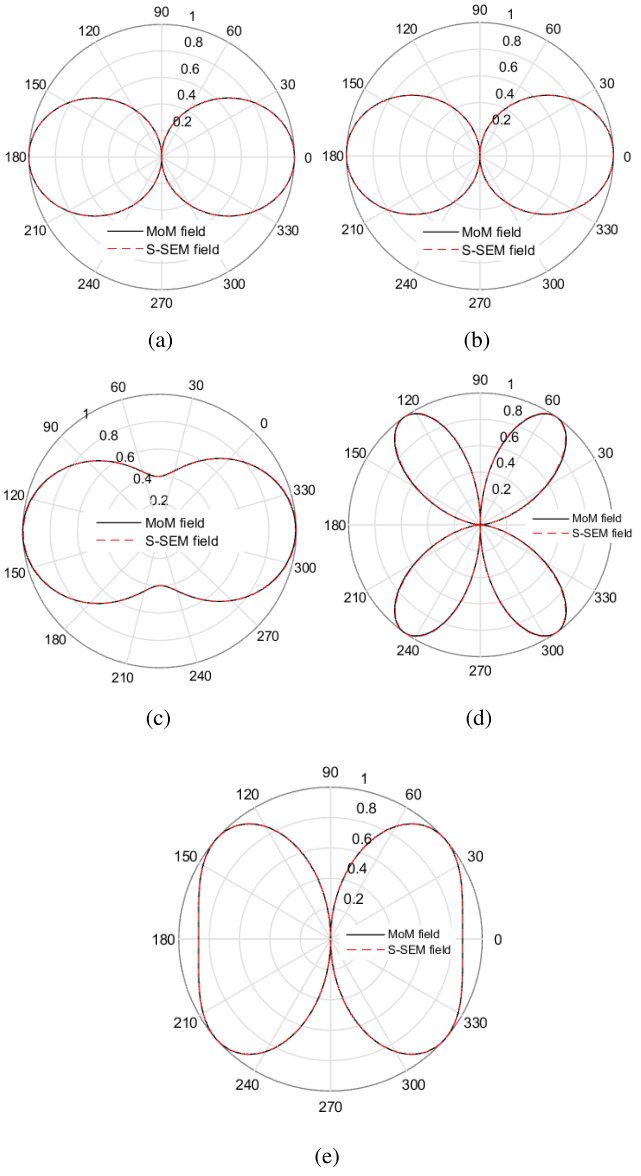

FIGURE 9. A comparison of far field polar plot in transmitting mode setup with respect to elevation angle θ between WIPL-D MoM code and the spatial-SEM approach. (a) Symmetric wire. (b) Asymmetric wire. (c) L-shaped wire. (d) Two-element array. (e) Three-element array.

of half wavelength each. The total number of S-SEM wires needed to model the system is six and the obtained S-SEM data are shown in Table 5. The general far-field array formula (57) was used then to predict the array field, and the results reported in Fig. 9. The agreement with MoM found there confirms that the S-SEM far-field theory allows direct and simple analytical predicting of the far-field for general wire array structures. For simplicity, in both two- and three-elements arrays, the excitation signals are all equated to 1V.

VIII. CONCLUSION

We presented a general formulation of the Singularity Expansion Method (SEM) applied to frequency-domain spatial

electromagnetic signals (via the Antenna Current Green's Function or ACGF) in contrast to the conventional time-domain formulation. The resulting spatial-SEM theory was extended to include the far field and exact analytical expression of the radiation pattern in terms of the SEM data were found, leading to the discovery of new sets of radiation and current modes through this method, which can be deployed as bases to expand any current/radiation pattern. The method has been confirmed by direct comparison between the newly derived analytical expressions and accurate full-wave MoM solution. It was found that the new S-SEM radiation modes computed by theory and the MoM predictions are in complete agreement. The examples include single wires, with both symmetric and asymmetric excitation, and also bent wires and wire arrays. Although the numerical examples involved wire structures, the proposed S-SEM algorithm is developed for the full-generic case of three-dimensional radiating objects. Moreover, the method can be extended to scattering problems.

The S-SEM method possesses the major advantage of being a frequency-domain approach, leading to the ability to work with only single-frequency data. Moreover, it was found that the notorious problem of how to separate the early- and late- time responses, which usually hinders temporal SEM applications, is completely absent in the spatial SEM algorithm. Based on the new connection between the S-SEM current distribution and the far-field, this can lead to new applications given that frequency-domain measurement is much easier than time time-domain measurements. The analytically-expressed current/radiation modal connection unearthed via the spatial-SEM can be harnessed to develop new generations of new inverse modeling algorithms suitable for radar target identification and sensor inverse modeling. Moreover, the simple analytical relation between the S-SEM data of the radiating current and the corresponding radiated fields allows efficient calculations of fields in complex array configurations, which could be used, for instance, to speed up simulations involving statistical analysis and optimization that requires extensive numerical computations of the far fields.

Finally, and most importantly, the spatial SEM formalism closes a gap in the current electromagnetic literature, which tends to focus heavily on the temporal (ω-type spectral analysis) composition of electromagnetic signals, by shedding more light this time on the spatio-frequency structure of electromagnetic fields and currents as a step toward a complete spatio-temporal spectral SEM theory. We believe that the proposed theory and its computational implementation for wire problems (fully developed here) and 2D patches (given in outline form here) will play a role in the next generation of fundamental and applied electromagnetic research.

REFERENCES

[1] C. E. Baum, "On the singularity expansion method for the solution of electromagnetic interaction problems," U.S. Air Force Res., EMP Appl. Note 8, 1971.

[2] C. Baum, "Emerging technology for transient and broad-band analysis and synthesis of antennas and scatterers," *Proc. IEEE*, vol. 64, no. 11, pp. 1598–1616, Nov. 1976.

[3] C. E. Baum, "The singularity expansion method," in *Transient Electromagnetic Fields*. New York, NY, USA: Springer-Verlag, 1976, pp. 129–179.

[4] C. E. Baum, "Signature-based target identification and pattern recognition," *IEEE Antennas Propag. Mag.*, vol. 36, no. 3, pp. 44–51, Jun. 1994.

[5] C. E. Baum, E. J. Rothwell, Y. F. Chen, and D. P. Nyquist, "The singularity expansion method and its application to target identification," *Proc. IEEE*, vol. 79, no. 10, pp. 1481–1492, Oct. 1991.

[6] C. E. Baum, "The forward-scattering theorem applied to the scattering dyadic," *IEEE Trans. Antennas Propag.*, vol. 55, no. 6, pp. 1488–1494, Jun. 2007.

[7] C. Baum, *The Singularity Expansion Method In Electromagnetics: A Summary Survey And Open Questions*. Morrisville, NC, USA: Lulu Enterprises, Inc, 2012.

[8] E. Heyman and L. B. Felsen, "A wavefront interpretation of the singularity expansion method," *IEEE Trans. Antennas Propag.*, vol. AP-33, no. 7, pp. 706–718, Jul. 1985.

[9] D. Riley, W. Davis, and I. Besieris, "The singularity expansion method and multiple scattering," *Radio Sci.*, vol. 20, no. 1, pp. 20–24, 1985.

[10] P. R. Barnes, "On the singularity expansion method as applied to the EMP analysis and simulation of the cylindrical dipole antenna," U.S. Air Force Res., EMP Appl. Note 146, Nov. 1973.

[11] A. G. Ramm, "Theoretical and practical aspects of singularity and eigenmode expansion methods," *IEEE Trans. Antennas Propag.*, vol. AP-28, no. 6, pp. 897–901, Nov. 1980.

[12] A. G. Ramm, "Mathematical foundations of the singualarity and eigenmode expansion methods," *J. Math. Anal. Appl.*, vol. 86, no. 2, pp. 562–591, 1982.

[13] M. A. Morgan, "Singularity expansion representations of fields and currents in transient scattering," *IEEE Trans. Antennas Propag.*, vol. AP-32, no. 5, pp. 466–473, May 1984.

[14] L. Marin, "Natural-mode representation of transient scattered fields," *IEEE Trans. Antennas Propag.*, vol. AP-21, no. 6, pp. 809–818, Nov. 1973. doi: 10.1109/TAP.1973.1140603.

[15] F. Tesche, "On the analysis of scattering and antenna problems using the singularity expansion technique," *IEEE Trans. Antennas Propag.*, vol. AP-21, no. 1, pp. 53–62, Jan. 1973.

[16] F. Tesche, "The far-field response of a step-excited linear antenna using SEM," *IEEE Trans. Antennas Propag.*, vol. AP-23, no. 6, pp. 834–838, Nov. 1975.

[17] T. T. Crow, B. D. Graves, and C. D. Taylor, "The singularity expansion method as applied to perpendicular crossed wires," *IEEE Trans. Antennas Propag.*, vol. AP-23, no. 4, pp. 540–546, Jul. 1975.

[18] K. R. Umashankar, T. H. Shumpert, and D. R. Wilton, "Scattering by a thin wire parallel to a ground plane using the singularity expansion method," *IEEE Trans. Antennas Propag.*, vol. AP-23, no. 2, pp. 178–184, Mar. 1975.

[19] J. T. Cordaro and W. A. Davis, "Time-domain techniques in the singularity expansion method," *IEEE Trans. Antennas Propag.*, vol. AP-29, no. 3, pp. 534–538, May 1981.

[20] C. Dolph and S. Cho, "On the relationship between the singularity expansion method and the mathematical theory of scattering," *IEEE Trans. Antennas Propag.*, vol. AP-28, no. 6, pp. 888–897, Nov. 1980.

[21] M. S. Aly and T. T. Y. Wong, "Early-time scattered field by perfectly conducting sphere using asymptotically compensated singularity expansion method," *Electron. Lett.*, vol. 25, no. 16, pp. 1066–1067, Aug. 1989.

[22] J. E. Ross, E. J. Rothwell, D. P. Nyquist, and K. M. Chen, "Approximate integral-operator methods for estimating the natural frequencies of coupled objects," *Radio Sci.*, vol. 29, pp. 677–684, Jul./Aug. 1994.

[23] J. E. Ross, E. J. Rothwell, D. Nyquist, and K.-M. Chen, "Transient coupling analysis using the singularity expansion method," *IEEE Trans. Electromagn. Compat.*, vol. 36, no. 4, pp. 358–364, Nov. 1994.

[24] Q. Li, P. Ilavarasan, J. E. Ross, E. J. Rothwell, Y. F. Chen, and D. P. Nyquist, "Radar target identification using a combined early-time/late-time E-pulse technique," *IEEE Trans. Antennas Propag.*, vol. 46, no. 9, pp. 1272–1278, Sep. 1998.

[25] S. Licul and W. A. Davis, "Unified frequency and time-domain antenna modeling and characterization," *IEEE Trans. Antennas Propag.*, vol. 53, no. 9, pp. 2882–2888, Sep. 2005.

[26] J. Yang and T. K. Sarkar, "Interpolation/extrapolation of radar cross section (RCS) data in the frequency domain using the Cauchy method," *IEEE Trans. Antennas Propag.*, vol. 55, no. 10, pp. 2844–2851, Oct. 2007.

[27] F. Aldhubaib, N. V. Shuley, and H. S. Lui, "Characteristic polarization states in an ultrawideband context based on the singularity expansion method," *IEEE Trans. Geosci. Remote Sens. Lett.*, vol. 6, no. 4, pp. 792–796, Oct. 2009.
[28] R. Rezaiesarlak and M. Manteghi, "Complex-natural-resonance-based design of chipless RFID tag for high-density data," *IEEE Trans. Antennas Propag.*, vol. 62, no. 2, pp. 898–904, Feb. 2014.
[29] R. Rezaiesarlak and M. Manteghi, "Accurate extraction of early-/late-time responses using short-time matrix pencil method for transient analysis of scatterers," *IEEE Trans. Antennas Propag.*, vol. 63, no. 11, pp. 4995–5002, Nov. 2015.
[30] J. Chauveau, N. De Beaucoudray, and J. Saillard, "Selection of contributing natural poles for the characterization of perfectly conducting targets in resonance region," *IEEE Trans. Antennas Propag.*, vol. 55, no. 9, pp. 2610–2617, Sep. 2007.
[31] C. Marchais, B. Uguen, A. Sharaiha, G. L. Ray, and L. Le Coq, "Compact characterisation of ultra wideband antenna responses from frequency measurements," *IET Microw. Antennas Propag.*, vol. 5, no. 6, pp. 671–675, 2011.
[32] W. Lee, T. K. Sarkar, H. Moon, and M. Salazar-Palma, "Computation of the natural poles of an object in the frequency domain using the cauchy method," *IEEE Antennas Wireless Propag. Lett.*, vol. 11, pp. 1137–1140, Apr. 2012.
[33] F. Sarrazin, J. Chauveau, P. Pouliguen, P. Potier, and A. Sharaiha, "Accuracy of singularity expansion method in time and frequency domains to characterize antennas in presence of noise," *IEEE Trans. Antennas Propag.*, vol. 62, no. 3, pp. 1261–1269, Mar. 2014.
[34] B. Kolundzija and A. Djordjevic, *Electromagnetic Modeling of Composite Metallic and Dielectric Structures*. Norwood, MA, USA: Artech House, 2002.
[35] T. B. Hansen and A. D. Yaghjin, *Plane-Wave Theory Time-Domain Fields*. Piscataway, NJ, USA: IEEE Press, 1999.
[36] S. M. Mikki and Y. M. M. Antar, "Analysis of electromagnetic interactions in antenna arrays using the antenna current Green's function method," in *Proc. IEEE Antennas Propag./URSI Int. Symp.*, 2011.
[37] S. M. Mikki and Y. M. M. Antar, "On the fundamental relationship between the transmitting and receiving modes of general antenna systems: A new approach," *IEEE Antennas Wireless Commun. Lett.*, vol. 11, pp. 232–235, 2012.
[38] S. M. Mikki and Y. M. M. Antar, "The antenna current Green's function formalism—Part I," *IEEE Trans. Antennas Propag.*, vol. 61, no. 9, pp. 4493–4504, Sep. 2013.
[39] S. M. Mikki and Y. M. M. Antar, "The antenna current Green's function formalism—Part II," *IEEE Trans. Antennas Propag.*, vol. 61, no. 9, pp. 4505–4519, Sep. 2013.
[40] S. Henault, S. K. Podilchak, S. M. Mikki, and Y. M. M. Antar, "A general methodology for mutual coupling estimation and compensation," *IEEE Trans. Antennas Propag.*, vol. 16, no. 3, pp. 1119–1131, Mar. 2013.
[41] F. Sarrazin, S. Mikki, Y. Antar, P. Pouliguen, and A. Sharaiha, "Study of dipole antennas' characteristic modes through the antenna current Green's function and the singularity expansion method," in *Proc. EuCap*, Lisbon, Portugal, Apr. 2015, pp. 1–2.
[42] S. M. Mikki and Y. M. M. Antar, "Analysis of generic near-field interactions using the antenna current Green's function," *Prog. Electromagn. Res. C*, vol. 59, pp. 1–9, 2015.
[43] S. M. Mikki and Y. M. M. Antar, *New Foundations for Applied Electromagnetics*. Norwood, MA, USA: Artech House, 2016.
[44] A. M. Alzahed, S. M. Mikki, Y. M. M. Antar, M. Clénet, and S. Jovic, "Characterization of a rectangular patch antenna using ACGF-SEM approach," in *Proc. IEEE Conf. Antenna Meas. Appl. (CAMA)*, Syracuse, NY, USA, Oct. 2016, pp. 1–3.
[45] A. M. Alzahed, S. Mikki, Y. Antar, M. Clénet, S. Jovic, "The ACGF-SEM approach to electromagnetic radiation with applications in radar and inverse modeling," in *Proc. Int. Union Radio Sci. General Assem. Sci. Symp. (URSI)*, Montréal, QC, USA, Aug. 2017.
[46] A. M. Alzahed, S. M. Mikki, and Y. M. M. Antar, "An innovative method of mutual coupling compensation for DOA estimation," in *Proc. IEEE Conf. Antenna Technol. Appl. Electromagn. (ANTEM)*, Montréal, QC, USA, Jul. 2016, pp. 1–4.
[47] R. F. Harrington and J. R. Mautz, "Theory of characteristic modes for conducting bodies," *IEEE Trans. Antennas Propag.*, vol. AP-19, no. 5, pp. 622–628, Sep. 1971.
[48] T. Y. Chen and C.-F. Wang, *Characteristic Modes: Theory and Applications in Antenna Engineering*. Hoboken, NJ, USA: Wiley, 2015.
[49] W. C. Chew, *Waves and Fields in Inhomogenous Media*. Hoboken, NJ, USA: Wiley, 1999.
[50] A. S. Schelkunoff, *Electromagnetic Waves*. Princton, NJ, USA: Van Nostrand, 1943.
[51] A. S. Schelkunoff and T. H. Friis, *Antennas: From Theory to Practice*. New York, NY, USA: Wiley, 1952.
[52] G. C. Someda, *Electromagnetic Waves*. London, U.K.: Chapman & Hall, 1998.
[53] I. V. Lindell, *Methods for Electromagnetic Field Analysis*. Hoboken, NJ, USA: Wiley, 1996.
[54] J. V. Bladel, *Electromagnetic Fields*. Hoboken, NJ, USA: Wiley, 2007.
[55] R. S. Elliott, *Antenna Theory & Design*. Hoboken, NJ, USA: Wiley, 2002.
[56] A. C. Balanis, *Antenna Theory: Analysis and Design*, 3rd ed. Hoboken, NJ, USA: Wiley, 2005.
[57] C. W. Gibson, *The Method of Moments in Electromagneticss*. London, U.K.: Chapman & Hall, 2008.
[58] R. F. Harrington, *Field Computation by Moment Methods*. New York, NY, USA: Macmillan, 1968.
[59] A. Kirsch and F. Hettlich, *The Mathematical Theory of Time-Harmonic Maxwell's Equations: Expansion-, Integral-, and Variational Methods*. Berlin, Germany: Springer, 2015.
[60] J.-C. Nedelec, *Acoustic and Electromagnetic Equations: Integral Representations for Harmonic Problems*. Berlin, Germany: Springer, 2001.
[61] W. C. Chew, M. S. Tong, and B. Hu, *Integral Equation Methods for Electromagnetic and Elastic Waves*. San Rafael, CA, USA: Morgan & Claypool, 2009.
[62] L. B. Felsen and N. Marcuvitz, *Radiation and Scattering of Waves*. Piscataway, NJ, USA: IEEE Press, 1994.
[63] J. Schwinger, *Classical Electroynamics*. Boulder, CO, USA: Westview, 1998.
[64] J. D. Jackson, *Classical Electrodynamics*, 3rd ed. New York, NY, USA: Wiley.
[65] A. Zangwill, *Modern Electrodynamics*. Cambridge, U.K.: Cambridge Univ. Press, 2017.
[66] A. Garg, *Classical Electromagnetism in a Nutshell*. Princeton, NJ, USA: Princeton Univ. Press,, 2012.
[67] R. Prony, "Essai expérimental et analytique sur les lois de la Dilatabilité des fluides élastiques et sur celles de la Force expansive de la vapeur de l'eau et la vapeur de l'alkool," *J. l'cole Polytechnique*, vol. 1, no. 22, pp. 24–80, 1795.
[68] Y. Hua and T. K. Sarkar, "Generalized pencil-of-function method for extracting poles of an EM system from its transient response," *IEEE Trans. Antennas Propag.*, vol. 37, no. 2, pp. 229–234, Feb. 1989.
[69] Y. Hua and T. K. Sarkar, "Matrix pencil method for estimating parameters of exponentially damped/undamped sinusoids in noise," *IEEE Trans. Acoust., Speech, Signal Process.*, vol. 38, no. 5, pp. 814–824, May 1990.
[70] S. Yang, Y. Kim, H. Jo, and N. Myung, "Alternative method for obtaining antenna current Green's function based on infinitesimal dipole modeling," *IEEE Trans. Antennas Propag.*, vol. 67, no. 4, pp. 2583–2590, Apr. 2019. doi: 10.1109/TAP.2019.2894279.

SAID MIKKI received the Ph.D. degree in electrical engineering from The University of Mississippi, in 2008. From 2009 to 2015, he was a Research Fellow with the Electrical and Computer Engineering Department, Royal Military College of Canada, ON, Canada. In 2015, he joined the Electrical and Computer and Computer Science Department, University of New Haven, West Haven, CT, USA. He has published in the areas of fundamental electromagnetic theory, computational methods, and optimization techniques in electromagnetics, nano-electrodynamics, metamaterials, antenna near fields, and novel methods for characterizing antenna systems, including antenna synthesis algorithms and designs. In 2016, he has published *New Foundations for Applied Electromagnetics: Spatial Structures of Fields* (London and Boston: Artech House, 2016). His current research interests include wireless communications, electromagnetic theory, antennas and circuits, machine learning and artificial intelligence, quantum information processing, and nanotechnology.

ABDELELAH M. ALZAHED is currently pursuing the Ph.D. degree with the Royal Military College of Canada. His research interests include electromagnetics, signal processing, optimization, antennas, and high-frequency circuits.

YAHIA M. M. ANTAR (S'73–M'76–SM'85–LF'00) received the B.Sc. degree (Hons.) in electrical engineering from Alexandria University, Alexandria, Egypt, in 1966, and the M.Sc. and Ph.D. degrees in electrical engineering from the University of Manitoba, MB, Canada, in 1971 and 1975, respectively.

In 1987, he joined the Department of Electrical and Computer Engineering, Royal Military College of Canada, Kingston, where he has been a Professor, since 1990. He has a cross appointment with Queen's University, Kingston. He has authored or co-authored over 200 journal papers, several books and chapters in books, over 450 refereed conference papers, and holds several patents. He is a Life Fellow of the Institute of Electrical and Electronic Engineers (IEEE) and a Fellow of the Engineering Institute of Canada, the Electromagnetic Academy, and the International Union of Radio Science. In 2011, he was appointed as a member of the Canadian Defence Advisory Board, Canadian Department of National Defence. He has supervised and co-supervised over 90 Ph.D. and M.Sc. dissertations with the Royal Military College and Queen's University, several of which have received the Governor General of Canada Gold Medal Award, the Outstanding Ph.D. Thesis of the Division of Applied Science, and many best paper awards in major international symposia. He was a recipient of the Royal Military College of Canada Excellence in Research Prize, in 2003, the RMCC Class of 1965 Teaching Excellence Award, in 2012, the 2014 IEEE Canada RA Fessenden Silver Medal for Ground Breaking Contributions to Electromagnetics and Communications, the 2015 IEEE Canada J. M. Ham Outstanding Engineering Education Award, and the Royal Military College of Canada Cowan Prize for excellence in research, in 2015. He received the Queen's Diamond Jubilee Medal from the Governor General of Canada in recognition for his contribution to Canada, in 2012, and the Chen-To-Tai Distinguished Educator Award from the IEEE-AP-S, in 2017. In 2002, he was awarded the Tier 1 Canada Research Chair in Electromagnetic Engineering which has been renewed, in 2016. He was elected by the URSI to the Board as a Vice President, in 2008 and 2014, and to the IEEE AP AdCom., in 2009. In 1977, he joined the Communications Research Centre, Ottawa, as a Government of Canada Visiting Fellow. In 1979, he joined the Division of Electrical Engineering, National Research Council of Canada. He has served as the Chair for CNC, URSI, from 1999 to 2008, and Commission B, from 1993 to 1999. He has chaired several national and international conferences and has given plenary talks in many conferences. He serves as an Associate Editor for many IEEE and IET journals and as an IEEE-APS Distinguished Lecturer.